Cell transplantation and gene therapy approaches for the treatment of retinal degenerative disorders

DISSERTATION

zur Erlangung des akademischen Grades

Doctor rerum naturalium

(Dr. rer. nat.)

vorgelegt

der Fakultät Mathematik und Naturwissenschaften der Technischen Universität Dresden

von

Dipl. biol. Dominic Eberle

geboren am 22.08.1983 in Neuhaus am Rennweg

Eingereicht am 05.09.2012

Die Dissertation wurde in der Zeit von Oktober 2008 bis September 2012 am Zentrum für Regenerative Therapien, TU Dresden angefertigt.

Gutachter: Prof. Elly Tanaka, Prof. Udo Bartsch

Datum der Verteidigung: 21.12.2012

Table of Contents

1) Introduction

„To suppose that the eye, with all its inimitable contrivances for adjusting the focus to different distances, for admitting different amounts of light, and for the correction of spherical and chromatic aberration, could have been formed by natural selection, seems, I freely confess, absurd in the highest possible degree. Yet reason tells me, that if numerous gradations from a perfect and complex eye to one very imperfect and simple, each grade being useful to its possessor, can be shown to exist; if further, the eye does vary ever so slightly, and the variations be inherited, which is certainly the case; and if any variation or modification in the organ be ever useful to an animal under changing conditions of life, then the difficulty of believing that a perfect and complex eye could be formed by natural selection, though insuperable by our imagination, can hardly be considered real. How a nerve comes to be sensitive to light, hardly concerns us more than how life itself first originated; but I may remark that several facts make me suspect that any sensitive nerve may be rendered sensitive to light, and likewise to those coarser vibrations of the air which produce sound.“

Charles Darwin, On The Origin of Species, Chapter Six, "Organs of Extreme Perfection and Complication"

In his book “The Origin of Species“ (1859), Charles Darwin highlighted the eye within the group of “organs of extreme perfection and complication” [1]. Through all of his studies he found evidence for the evolution of organs and animals but impressed by the complexity and perfection of the eye he used it as an example that even unimaginably complex things could have been evolved. Today the evolution of the eye is an established and proven theory, well investigated, though not concluded.

The human eye is one of the most complex within the animal kingdom. It is composed of different layers, structures and cell types each unique in its morphology and function (Fig. 1). The cornea is the frontal transparent surface of the anterior eye chamber, protecting the fluid in this chamber, the lens and the iris. The sclera is the “white surface“ protecting the rest of the eyeball. Together, they form the outer layer of the eye. The

intermediate layer is composed of the choroid, harboring the blood drainage of the eye, and the ciliary body, where muscles are found which attach to the zonule fibers attaching the lens. Contraction and relaxation of these muscles induces shape changes of the lens, allowing accommodation, the sharpening of points in different distances. The neuronal inner layer is named retina (Fig. 2). Here we find several specialized cell types, enabling this part of the eye to detect light (rod and cone photoreceptors), transform it into electric signals, process it further via second order neurons (horizontal, bipolar and amacrine cells) and transduce it towards the visual cortex of the brain (ganglion cells). Other cell types perform regulatory maintenance (retinal pigment epithelial and Müller glia cells) and immunogenic tasks (microglia cells).

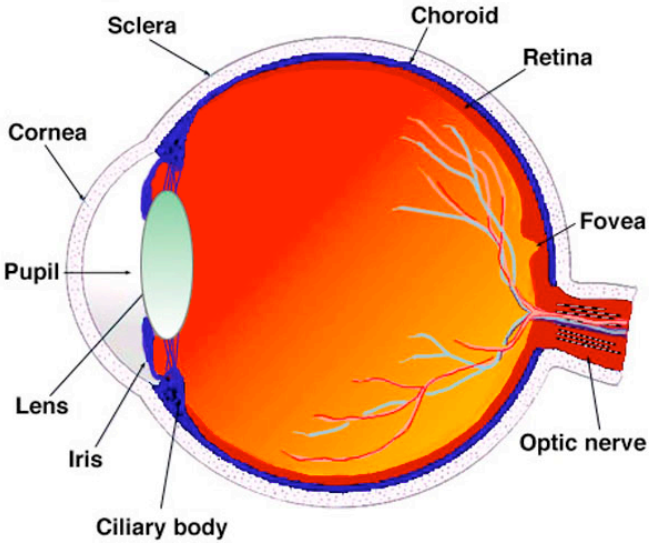

Figure 1: Schematic drawing of the human eye. Adapted from http://webvision.med.utah.edu/

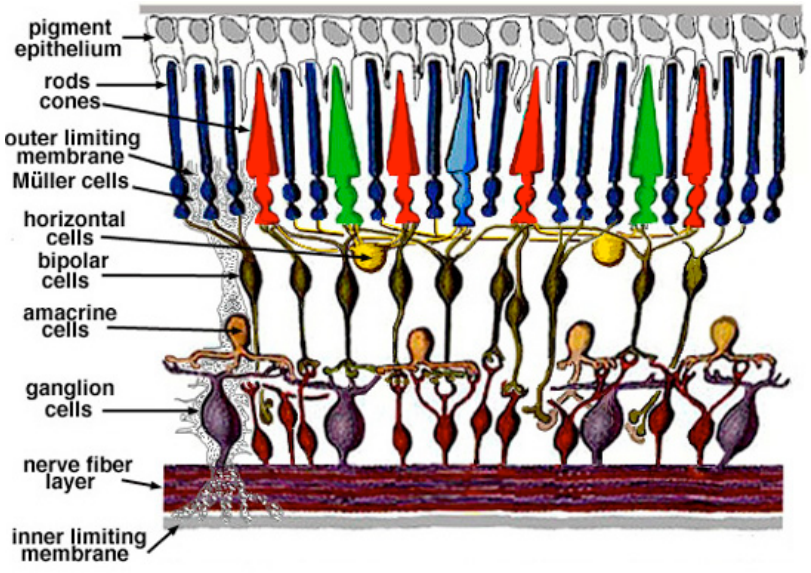

Figure 2: Schematic drawing of the vertebrate retina. Adapted from http://webvision.med.utah.edu/

The human retina harbors 92 million rods and 4.6 million cones which are in total almost 100 million light sensing cells per eye [2]. With an area of 1094 mm^2 , the human retina features an average density of ~90 photoreceptors per μm^2 peaking in a special region of the primate retina, the fovea, with ~170 cones / μm^2, whereas the rod density was reported to be ~80 - 100 rods / μm^2 (see http://webvision.med.utah.edu/). These highly sensitive rod photoreceptor cells, which contain the visual pigment rhodopsin, are responsible for monochromatic vision under dim light conditions. In contrast, cone photoreceptor cells, which contain S-, M-, or L-opsins enable trichromatic vision under normal daylight conditions ([3] and Tab. 1). Both photoreceptors feature an outer segment (OS) where the light is detected by the visual pigments, localized in repetitive membrane staples (Fig. 3). The OSs are directed towards the retinal pigment epithelial (RPE) cell layer (Fig. 2). The connecting cilium (CC) is the link between the OS and the inner segment (IS), containing the majority of the mitochondria (mt) of the cell (Fig. 3). Towards the inner retina, a cell membrane tunnel connects the IS with the main cell body, containing the nucleus (nuc). In rods, the nucleus displays a characteristic condensed chromatin structure whereas in cones several condensed spots of heterochromatin can be observed [4]. Additionally, cone nuclei could be found predominantly in the outer part of the outer nuclear layer (ONL) as indicated in Fig. 3. After detection of light in the OS, an electric current is triggered which is transduced via the IS and the nucleus towards the axonal terminal (AT) which projects into the outer limiting membrane (OLM) (Fig. 3). There, the signal is picked up by bipolar and horizontal cells, processed and transduced further via retinal ganglion cells (RGCs) towards the brain. A small sub-population of RGCs, the so called intrinsically photosensitive RGCs (ipRGCs), represent, next to rods and cones, a third population of light-detecting mammalian retinal neurons. While rods and cones react on short timescales within milliseconds, ipRGCs seem to be responsible for light-sensing actions on longer

timescales, like synchronization of circadian rhythms, modulation of melatonin release and regulation of pupil size [5,6].

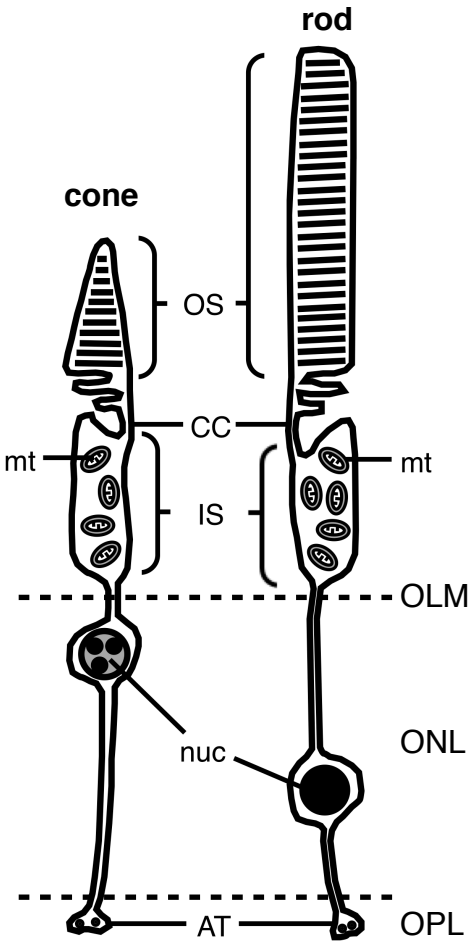

Light-detecting cell type	Visual pigment protein	Relative absorbance peak [nm]	Human	Mouse
Rods	Rhodopsin	498	✓	✓
S Cones (blue)	S - Opsin	437	✓	✓
M Cones (green)	M - Opsin	533	✓	✓
L Cones (red)	L - Opsin	564	✓	X
ipRGCs	Melanopsin	480	✓	✓

Table 1: Features of light-sensitive cell types in the human and mouse retina. Within the mammalian retina, 3 different light-sensing cell types could be found, rods, cones and intrinsically photosensitive retinal ganglion cells (ipRGCs). They are characterized by different visual pigment proteins which results in different absorbance spectra, enabling humans to have trichromatic vision while mice have only dichromatic vision **[3,6]**.

Figure 3 (left): Schematic drawing of a rod and cone photoreceptor cell. Incoming light is detected at the outer segments (OS) of cone and rod photoreceptor cells. The signal is translated into an electric current which is transduced further via the connecting cilium (CC) and the inner segment (IS), which harbors most of the mitochondria (mt) of the cell. Subsequently, the signal is transduced via an axon, the cell body which contains the nucleus and towards the axonal terminal (AT) where it is picked up by bipolar and horizontal cells.

Photoreceptors are of prime importance for humans, since vision is one of the most important senses for us. In our daily life, where nearly every action is dependent on visual input, an impairment or a loss of eyesight leads to severe disability.

With a non-syndromic prevalence of 1:4000, retinitis pigmentosa (RP), a collective term for a group of inherited retinal eye diseases, represents, together with age-related macula degeneration (AMD), one of the main causes for visual impairment and blindness in industrialized countries [7]. The dominant reason for vision loss is, in both cases, the irreversible loss of photoreceptor cells located in the ONL of the retina. To date, no effective treatment is available to preserve or regain visual function in affected patients.

Recent promising strategies for new retinal therapeutical approaches focus on one hand on the development of gene therapies, where an artificially introduced wt allele compensates a mutated gene, and on the other hand on cell therapies, where stem or photoreceptor precursor cells (PPCs) are transplanted to the sub-retinal space to replace degenerated host photoreceptors (Fig. 4). In comparison to ocular cell therapies, viral vector-mediated gene therapies for retinal degenerative diseases are relatively well investigated and some are already in clinical trial phases [8-10]. But their specificity limit their effectiveness to the level of mutations of single genes. Therefore, only subgroups of patients with retinal degenerative disorders may benefit from them. In contrast, the cell transplantational approach is still in its infancy. Nevertheless, a cell therapy implies a remarkable advantage. Retinal degenerative diseases with common phenotype, but a variety of genes that might be mutated, may be cured by introducing new, genetically native and healthy PPCs.

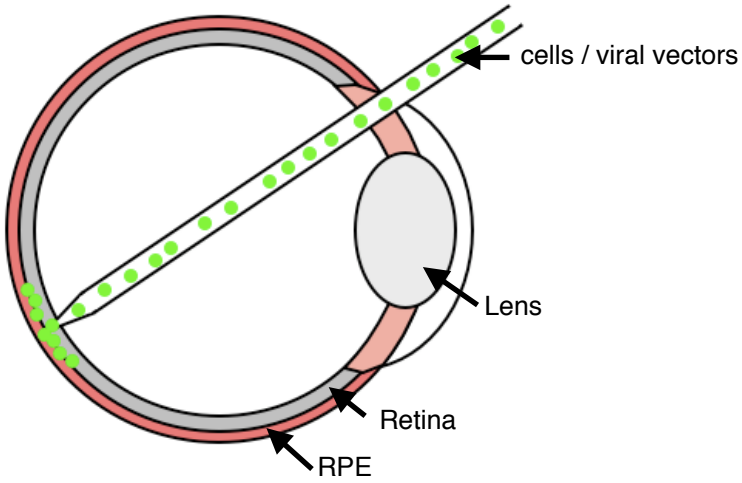

Figure 4: Schematic drawing of the principle of a sub-retinal injection. With sub-retinal injections, cells (for cell therapy) or viral vectors (for gene therapy) are delivered to the region between photoreceptor outer nuclear layer (ONL, the outermost region of the retina) and the retinal pigment epithelial cell layer (RPE) of a host animal. The injection needle is inserted through a small hole between sclera and cornea, navigated under visual control through the vitreus by avoiding the lens and placed behind the retina.

This study, which is subdivided into three parts, addresses the issue of non-reversible photoreceptor cell loss due to retinal degenerative diseases by investigating in the first two parts new qualitative as well as quantitative approaches in the field of retinal cell therapy. In the third part an ocular gene therapeutical approach targeting prominin-1, a gene involved in retinal degenerative disorders, was investigated.

2) Cell therapy: Increased integration of transplanted CD73-positive photoreceptor precursors into adult mouse retina

2.1) Introduction

Following up on initial studies by Peter Gouras et al. [11-13] already two decades ago, several recent reports demonstrated that transplantation of photoreceptor precursor cells (PPCs) into the sub-retinal space of adult mice results in integration into the host outer nuclear layer (ONL) and formation of mature rod and cone photoreceptors [14-17]. Importantly, donor cells correctly integrated and developed outer segments (OSs) located in the sub-retinal space and axonal terminals placed in the outer plexiform layer (OPL) in close proximity to endogenous bipolar cells, indispensable prerequisites for a functional connection to the host neural circuitry. Indeed, first studies suggested functionality of donor-derived photoreceptors as demonstrated by extracellular field potential recordings from the ganglion cell layer and pupillary reflexes [15], electro-retinography measurements [18] as well as patch-clamp recordings, optokinetic tracking, water-maze, and optical imaging from the visual cortex [19].

To date, several studies used heterogeneous cell suspensions generated by dissociation of entire retinae. Previous data indicate that cell suspensions from mouse retinae isolated between postnatal day (PN) 3 - 5 have the highest potential for integration [15,16]. Consistent for all published studies in which primary retinal cells were used for transplantation is the relatively low number of donor-derived photoreceptors that integrated into the ONL of the host. Various approaches have been performed to increase the number and survival of integrating photoreceptors including disruption of the outer limiting membrane [20,21], immune suppression [22], anti-apoptotic treatment of donor cells [23],

double-injection per eye, pre-detachment, scleral puncture [19] or enrichment of fluorescence reporter expressing donor cells by flow cytometry [17].

However, purification of transplantable cells based on the expression of reporter genes might not be an approach that can be used in possible future therapeutic applications in humans. Instead, it would be favorable to purify donor cells by cell-type specific cell surface markers. Such selection and enrichment methods will be specifically important when photoreceptor precursors are generated from an *in vitro* expandable cell source like pluripotent embryonic stem (ES) or induced pluripotent stem (iPS) cells. Current protocols allow the *in vitro* generation of rod and cone photoreceptors from mouse and human pluripotent stem cells albeit still in relative small quantities [18,24-27].

In this part, I show that ecto-5'-nucleotidase, a 70-kDa glycosyl-phosphatidylinositol (GPI)-anchored cell surface molecule, also called cluster of differentiation (CD) 73, is highly expressed in young rod photoreceptors confirming recent findings [28,29]. Furthermore, I demonstrate that magnetic-associated cell sorting (MACS) using antibodies against a cell surface antigen, i.e. CD73, is a reliable method for the enrichment of cells of the photoreceptor lineage. Importantly, upon transplantation purified suspensions of photoreceptor precursors showed a significantly increased integration rate into the ONL of adult mice when compared to unsorted or negative sorted cell fractions.

2.2) Results

2.2.1) Increased expression of CD73 in rod photoreceptors

Recent studies demonstrated that cell suspensions isolated from the mouse retina at post-natal day 3 to 5 have the highest integration rate after transplantation into the adult mouse retina [15-17]. Therefore, murine retinas used in this study for isolation of photoreceptors were dissected at PN4. To identify genes that are specifically up-regulated in young rod photoreceptors, microarray analysis was performed by Kai Postel to compare gene expression of rhoEGFP-positive and -negative cells isolated from PN4 mice. To further specify the profile of rhoEGFP-positive photoreceptors their gene expression was additionally compared to nestin-EGFP-positive cells isolated at PN0. Nestin, an intermediate filament protein, is highly expressed during retinal development and marks retinal progenitor cells. Microarray analysis revealed 8354 significantly changed entities (ANOVA; P = 0.05); 1125 entities showed more than a two-fold higher expression in rhoEGFP-positive cells in comparison to rhoEGFP-negative sorted cells (Fig. 5A) and nestin-EGFP-positive sorted cells (Fig. 5B). These 1125 entities represent 744 genes. The microarray data generated in this study have been published [30] and deposited in the National Center for Biotechnology Information's Gene Expression Omnibus (Bethesda, MD, [31]) and are accessible through GEO Series accession number GSE29318 (http://www.ncbi.nlm.nih.gov/geo/query/acc.cgi?acc=GSE29318).

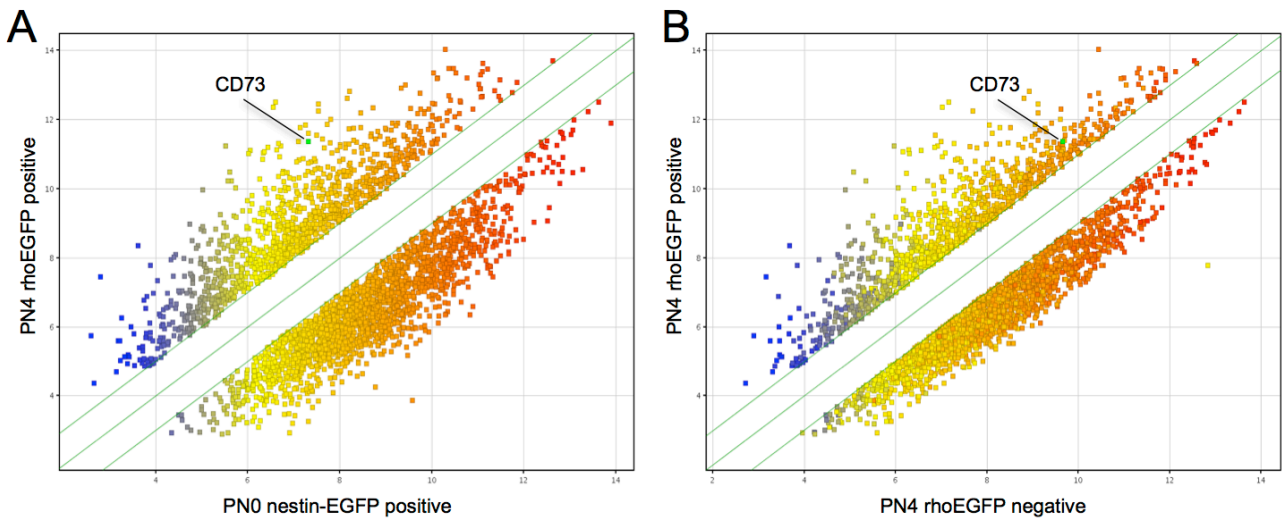

Figure 5: Comparison of the global expression profile of rhoEGFP positive cells versus rhoEGFP negative and nestin-EGFP positive cells. Scatter-plots of differentially expressed genes in PN4 rhoEGFP positive cells versus PN0 nestin-EGFP positive cells (A) and PN4 rhoEGFP positive versus PN4 rhoEGFP negative cells (B) revealed 2-fold gene expression differences (green lines) of 1125 up-regulated and 1948 down-regulated entities. CD73 is indicated by a green spot (A, B). Adapted from Eberle et al., 2011.

Several genes specific for the rod photoreceptor lineage — rhodopsin, Pde6b (phosphodiesterase subunit 6b), Gngt1 (guanine nucleotide binding protein (G protein) gamma transducing activity polypeptide 1), or recoverin — showed a more than 10-fold higher expression in rhoEGFP-positive cells, indicating the high selectivity of FACS enrichment for rod photoreceptors (Tab. 3). Microarray analysis also revealed genes encoding proteins located on the cell surface that may serve as antigens for antibody-mediated MACS. For example, CD73 (Nt5e, ecto- 5'-nucleotidase), Cnga1 (cyclic nucleotide gated channel alpha 1), Gje1 (gap junction protein, epsilon 3), and Pcdh15 (protocadherin 15) showed more than twofold higher expression in rhoEGFP PN4-positive cells compared with the other fractions (Fig. 5, Tab. 3). Altogether, 120 entities representing 79 different transcriptional units with GO-Term plasma membrane were identified and showed a more than twofold higher expression in PN4 rhoEGFP-sorted cells ([30] Supplementary Table S1, http://www.iovs.org/lookup/suppl/doi:10.1167/iovs.11-7399/-/DCSupplemental).

Gene Symbol	Gene Title	GO(Avadis)	Fold Change*
Photoreceptor Marker			
Rho	Rhodopsin	Photoreceptor activity	+++
Gngt1	Guanine nucleotide binding protein (G protein), gamma transducing activity polypeptide 1	Signal transducer activity	+++
Pde6b	Phosphodiesterase 6B, cGMP, rod receptor, beta polypeptide	3',5'-cyclic-GMP phosphodiesterase activity	++
Pde6g	Phosphodiesterase 6G, cGMP-specific, rod, gamma	cGMP binding	++
Rcvrn	Recoverin	Calcium ion binding	++
Cell Surface Marker			
Cnga1	Cyclic nucleotide gated channel alpha 1	cGMP binding	+++
Gje1	Gap junction protein, epsilon 1	Cell morphogenesis	++
Pcdh15	Protocadherin 15	Protein binding	+
Nt5e (CD73)	5' nucleotidase, ecto	Metal ion binding	+

* + 2-10 fold, ++ 10-20 fold, +++ ≥20 fold up-regulated respectively

Table 3: A subset of Genes with Higher Expression in PN4 rhoEGFP-Positive Cells in Comparison to PN4 rhoEGFP-Negative and PN0 Nestin-EGFP-Positive Cells. Adapted from Eberle et al., 2011.

Since the CD73 antibody was commercially available, we further focused on it in this study. Indeed, RT-PCR analysis perfomed by Sandra Schubert confirmed the expression of CD73 transcripts in PN4 mouse retina (Fig. 6C) and immunocytochemistry, using CD73-specific antibodies on dissociated and cultured rhoEGFP retinas showed CD73-immunoreactivity in the majority of GFP-positive rod photoreceptors ([30] Supplementary Fig. S1, http://www.iovs.org/lookup/suppl/doi:10.1167/iovs.11-7399/-/DCSupplemental). In line with our results, CD73 was recently identified as the first cell surface marker for early stages of the photoreceptor lineage after screening of several CD antigens [28]. Because of these findings we evaluated CD73 as the first candidate for proof-of-principle experiments investigating the transplantation of cell surface marker–enriched photoreceptors.

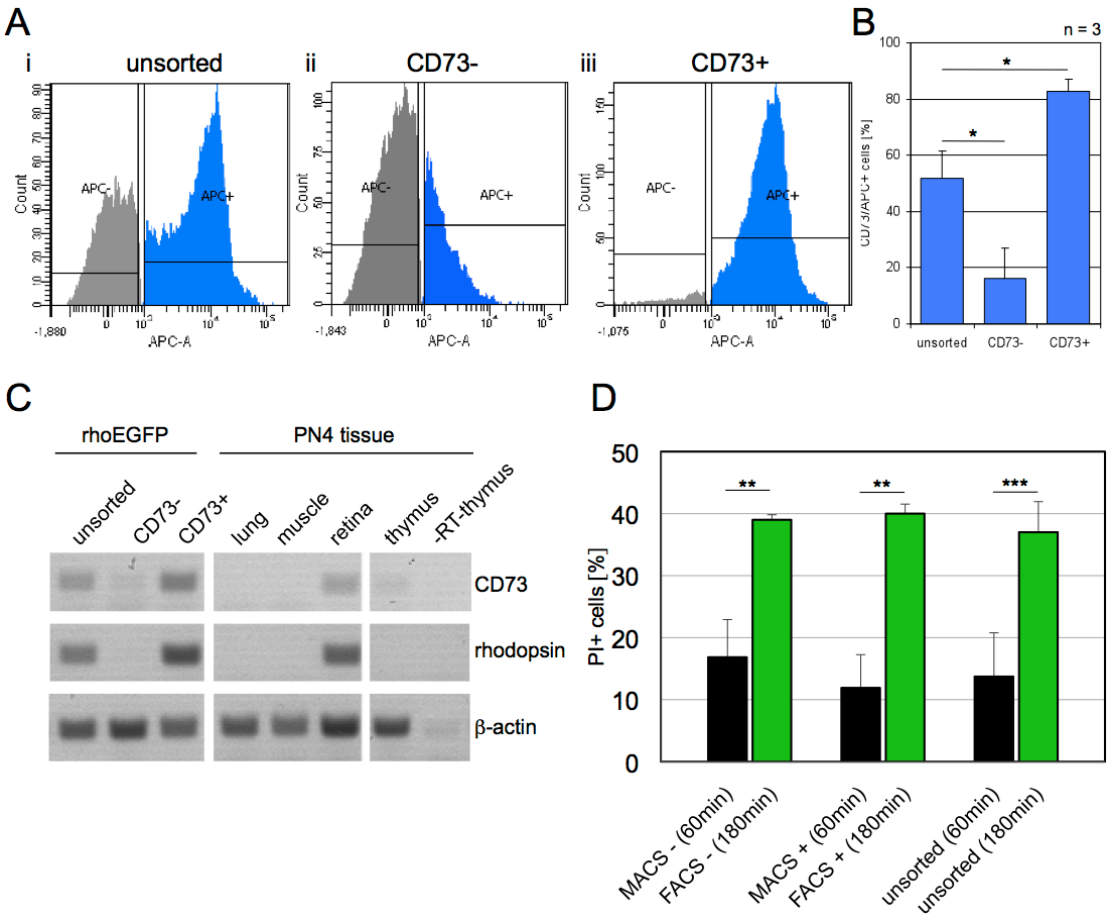

Figure 6: Analysis of unsorted, CD73-negative, and CD73-positive cells isolated from PN4 mouse retinas on MACS procedures. APC-conjugated secondary antibodies were used to detect CD73-positive cells after MACS. Unsorted cell fractions contained 52.0% ± 9.89% CD73-positive cells (Ai, B). After MACS, the number of CD73-positive cells was reduced to 16.0% ± 10.76% in CD73-negative sorted fractions (Aii, B) and increased to 83.0% ± 4.04% in positive sorted fractions (Aiii, B). Semiquantitative RT-PCR analysis using CD73-specific primers revealed CD73 expression in the PN4 mouse retina and CD73-positive cells (C). Using rhodopsin-specific primers, a strong expression of this rod photoreceptor marker was also detected in CD73-positive cells. Actin was used as internal control. Weak CD73 expression was also detected in the thymus (positive control), whereas lung and muscle served as negative controls beside thymus preparations without reverse transcriptase (– RT-thymus). Quantification of propidium iodide incorporation in PN4 retinal cells from rhoEGFP retinas after CD73 MACS or GFP FACS (D). In MACS propagated cells (MACS– and MACS+) an average of 15% showed incorporation of propidium iodide (PI), representing dead cells. The number of PI-positive cells was significantly increased in cells after flow cytometry (~37%; FACS– and FACS+). In comparing PI incorporation of unsorted cells after 60 or 180 minutes, similar proportions of PI-positive cells were detected (unsorted 60 minutes: 15% and unsorted 180 minutes: 37%). *P < 0.05, **P < 0.01, ***P < 0.001. Adapted from Eberle et al., 2011.

2.2.2) MACS enrichment of photoreceptor precursors

We further investigated whether CD73 antibodies are reliable tools for purification of cells of the photoreceptor lineage. Neural retina-specific leucine zipper (Nrl) is a transcription factor of the Maf subfamily and a critical regulator in photoreceptor final differentiation, expressed after cell cycle exit [32]. Without Nrl, the retina is devoid of rods, because all rod precursors transform into cone-like cells [32]. Therefore, Nrl is crucial for the differentiation of PPCs towards the rod lineage. In contrast, Cone-rod homeobox (Crx), another photoreceptor-specific transcription factor expressed earlier in development than Nrl and in rods and cones, is widely used as a marker for immature, post-mitotic photoreceptors. In this study, Nrl-EGFP and rhoEGFP transgenic mice are used as reporter to identify young rod photoreceptors in the retina.

In unsorted, CD73-MACS-negative, or CD73-MACS-positive cell fractions the number of EGFP-positive rod photoreceptors was analyzed by Sandra Schubert using flow cytometry and fluorescence microscopy after *in vitro* culturing. To test whether CD73-based MACS indeed results in enrichment of CD73-positive cells, Sandra Schubert first analyzed the number of CD73-positive cells in unsorted, CD73-negative and -positive sorted fractions by flow cytometry with APC-conjugated secondary antibodies. The results showed that unsorted cells contained 52% ± 9.89% CD73-positive cells (Figs. 6Ai, 6B) whereas negative fractions contained only 16% ± 10.76% (Figs. 6Aii, 6B). As anticipated, a strong increase—that is, 83% ± 4.04%, of CD73-positive cells was detected in the CD73-positive MAC- sorted fractions, confirming their successful enrichment by MACS (Figs. 6Aiii, 6B). Semiquantitative RT-PCR revealed also a strong expression of CD73 transcripts in CD73-positive sorted cells, whereas unsorted fractions and CD73-negative fractions showed moderate or low expression, respectively (Fig. 6C). Interestingly, RT-PCR analysis using rhodopsin-specific primers revealed a high expression of rhodopsin transcripts in

CD73- positive sorted fractions in contrast to CD73-negative ones, demonstrating the enrichment of rod photoreceptors (Fig. 6C).

The most common techniques for the enrichment of specific cell-types from heterogenous cell populations are either MACS or flow cytometry. In our hands, CD73-based MACS of retinas from one litter (6–10 pups) typically resulted in 20 to 30 million rhoEGFP-positive cells in ~60 minutes. In contrast, 4.4 to 7 million rhoEGFP-positive cells were isolated by flow cytometry with green fluorescence in ~180 minutes. To evaluate why MACS resulted in a higher number of cells, Sandra Schubert compared the effect of both techniques on the survival of the photoreceptor precursors. The number of dead cells was quantified by propidium iodide incorporation followed by flow cytometry. Whereas MAC-sorted cell fractions contained an average of 15% propidium iodide–positive cells, their number increased up to ~37% in the FAC-sorted fractions (Fig. 6D). Given that the time for high yield enrichment by flow cytometry was considerably longer, Sandra Schubert investigated whether the prolonged periods in suspension, rather than the sorting method itself, might be the underlying cause of the reduced number of cells obtained by FACS. Indeed, the analysis of unsorted cell suspensions 60 or 180 minutes after tissue dissociation revealed similar amounts of propidium iodide–positive cells (Fig. 6D). Thus, the increased cell death observed on flow cytometry appears to be due to the prolonged incubation periods, rather than the procedure itself. Consequently, all further experiments were performed with the fast and easy method, MACS.

By using retinas from Nrl-EGFP and rhoEGFP mice, Sandra Schubert next quantitatively investigated the enrichment of cells of the rod photoreceptor lineage by means of CD73-based MACS. FACS quantification showed that unsorted cell fractions contained 53% ± 5.25% Nrl-EGFP-positive (Figs. 7Ai, 7B) and 41% ± 3.35% rhoEGFP-positive (Figs. 7Ci, 7D) cells. In contrast, the CD73-positive cell fractions showed a significantly increased number of Nrl-EGFP- and rhoEGFP-positive cells, to 87% ± 6.33%

(Figs. 7Aiii, 7B) and 74% ± 9.95% (Figs. 7Ciii, 7D), respectively. Furthermore, in CD73-negative cell fractions the amount of Nrl-EGFP- and rhoEGFP-positive cells was strongly reduced (25.0% ± 2.96%; Figs. 7Aii, 7B; 6.0% ± 2.3%; Figs. 7Cii, 7D, respectively). In addition to the quantification of Nrl-EGFP- and rhoEGFP-positive cells from freshly isolated cells, the three separated cell fractions were further cultivated by Sandra Schubert *in vitro* for either 4 hours or 4 days. Immunocytochemistry on cultured cell fractions from rhoEGFP retinas after 4 days revealed a large number of CD73 - immuno-reactivity events in positive sorted cells, whereas their number in negative fractions was substantially reduced ([30] Supplementary Fig. S1, http://www.iovs.org/lookup/suppl/doi:10.1167/iovs.11-7399/-/DCSupplemental). Importantly, virtually all GFP-positive cells (rod photoreceptors) showed CD73 - immuno-reactivity, irrespective of the cell fraction analyzed ([30] Supplementary Fig. S1, http://www.iovs.org/lookup/suppl/doi:10.1167/iovs.11-7399/-/DCSupplemental). Quantification of *in vitro* propagated cell fractions showed also a significant increase in the number of Nrl-EGFP- and rhoEGFP-positive cells in the CD73-positive fractions by comparison to unsorted or negative ones (Fig. 7; [30] Supplementary Fig. S2, http://www.iovs.org/lookup/suppl/doi:10.1167/iovs.11-7399/-/DCSupplemental): 4 hours after MACS, the CD73-positive fractions contained 62.0% ± 4.56% Nrl-EGFP- positive (Fig. 7Ei) or 66.0% ± 3.42% rhoEGFP-positive (Fig. 7Fi) cells in comparison to unsorted cells (Nrl-EGFP, 23.0% ± 2.62%; rhoEGFP, 18% ± 0.99%) or CD73-negative cells (Nrl-EGFP, 2.0% ± 0.41%; rhoEGFP, 4.0% ± 1.21%; Figs. 7Ei, 7Fi). After 4 days in culture, similar proportions of EGFP-positive cells were detected for unsorted (Nrl-EGFP, 19.0% ± 0.62%; rhoEGFP, 10.0% ± 0.41%), negative (Nrl-EGFP, 2.0% ± 0.28%; rhoEGFP, 1.0% ± 0.34%), and positive (Nrl-EGFP, 53.0% ± 9.01%; rhoEGFP, 63.0% ± 2.71%) fractions (Figs. 7Eii, 7Fii), although with a slight decrease in all fractions in comparison to the 4-hour culturing time. Taken together, we could demonstrate

by using two independent EGFP-reporter lines that CD73 is a useful marker for enriching rod photoreceptor precursors via MACS.

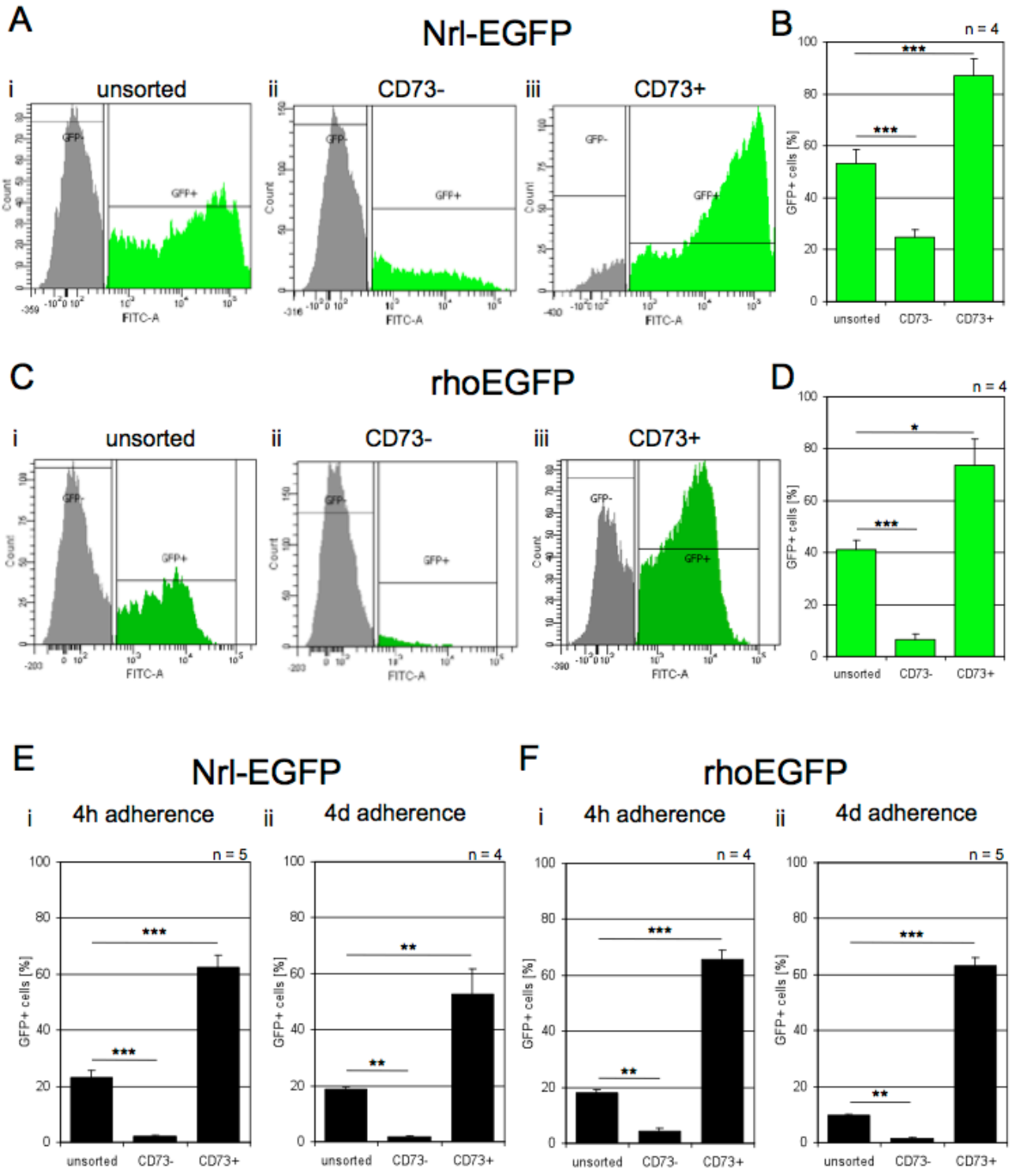

Figure 7: Analysis of unsorted, CD73-negative, and CD73-positive cells isolated from PN4 retinas after MACS. Quantification of dissociated retinal tissue from Nrl-EGFP mice by flow cytometry, directly after CD73-based MACS revealed a significant increase in GFP-positive cells in CD73-positive fractions (Aiii, B, CD73+) in comparison to unsorted cell fractions (Ai, B), whereas the number of GFP-positive cells

significantly decreased in CD73-negative fractions (Aii, B, CD73–). Similar results were obtained after quantification of cells isolated from rhoEGFP transgenic retinas (C, D). Note the higher number of GFP-negative cells in CD73-positive fractions sorted from rhoEGFP (Ciii) in comparison to Nrl-EGFP (Aiii) retinas. The number of GFP-positive cells was additionally quantified after *in vitro* culturing of CD73-sorted fractions on coverslips for 4 hours (Ei, Fi) or 4 days (Eii, Fii). CD73-positive fractions contained significantly higher amounts of GFP-positive cells in comparison to unsorted fractions from Nrl-EGFP (E) and rhoEGFP (F) transgenic retinas, whereas CD73-negative cells contained a significantly reduced number of GFP-positive cells (E, F) at both time points. n, number of experiments. *P < 0.05, **P < 0.01, ***P < 0.001. Adapted from Eberle et al., 2011.

2.2.3) Transplantation of enriched photoreceptor precursors

Promoter-driven expression of fluorescence reporters (as in Nrl-EGFP mice) results in cytoplasmic located reporter protein and strong labeling of the cell body of photoreceptors, including axonal terminals and inner segments. However, OS are only faintly stained in such reporter mice, and thus detailed analysis of OS formation of donor cells in high resolution is difficult to perform [16]. The fusion of EGFP to rhodopsin in rhoEGFP mice, in contrast, allows the detection and investigation of OS in more detail, as rhodopsin and thus EGFP are exclusively located in the OS disc membranes in mature photoreceptors [33]. Consequently, the cell body in mature photoreceptors of rhoEGFP mice are not labeled by the reporter (Fig. 8B). Thus, for all transplantation experiments, donor cells were isolated from rhoEGFP mice that additionally carried a ubiquitously expressed actin-DsRed transgene (Fig. 8) allowing simultaneous identification of integrated donor cells and formation of OS. Although the DsRed transgene was virtually expressed in all retinal cell types, the fluorescence signal intensity was highly variable. Of note, before the formation of OS during development (Fig. 8A) or after dissociation (Fig. 8C) young photoreceptors of rhoEGFP mice show EGFP expression located in the entire cell as could be also shown by immunocytochemistry using rhodopsin-specific antibodies ([30] Supplementary Figs. S3A–

C, http://www.iovs.org/lookup/suppl/doi:10.1167/iovs.11-7399/-/DCSupplemental). In addition, all GFP-positive cells from rhoEGFP retinas expressed recoverin, another photoreceptor marker ([30] Supplementary Figs. S3D–F, http://www.iovs.org/lookup/suppl/doi: 10.1167/iovs.11-7399/-/DCSupplemental).

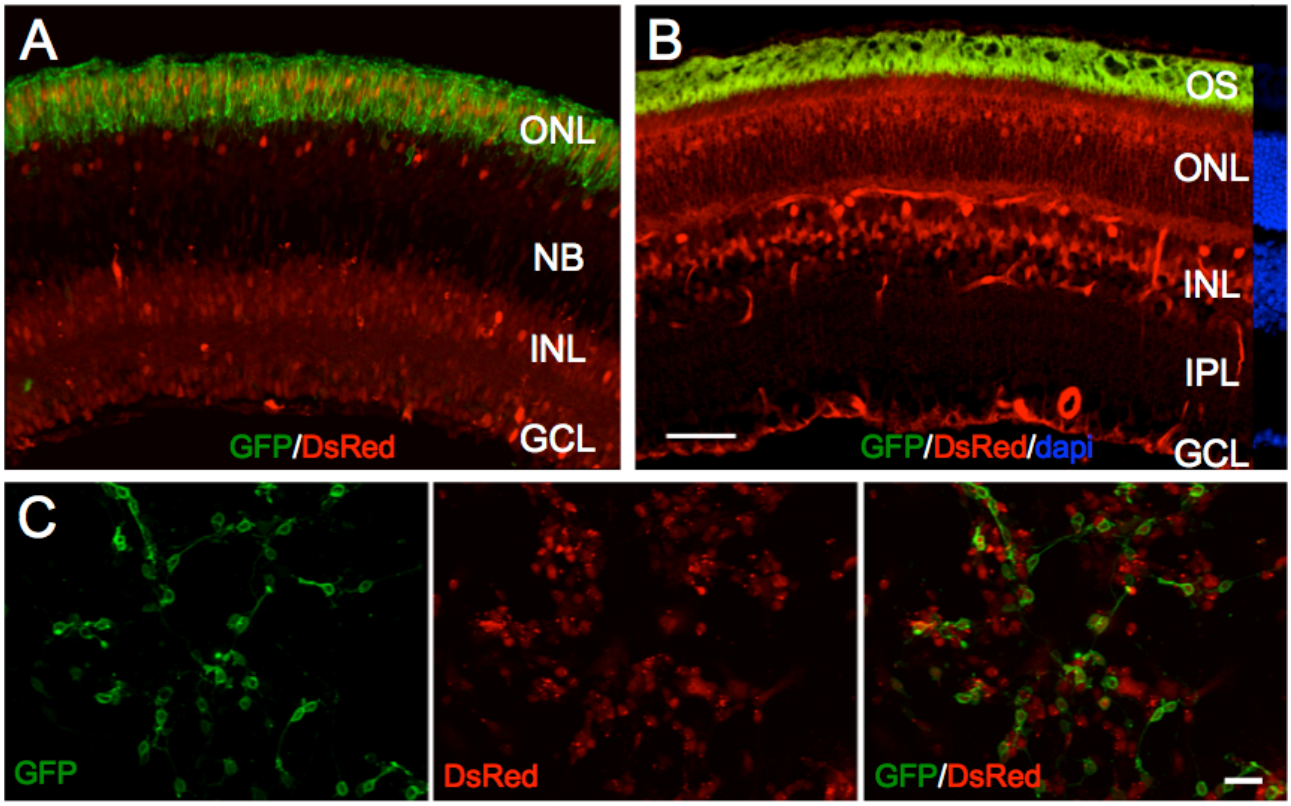

Figure 8: Reporter expression in rhoEGFP/DsRed double transgenic mice. Section of a rhoEGFP/DsRed retina at PN4 (A). All retinal cells show red fluorescence due to expression of DsRed albeit in different intensities. In the forming ONL, most of the cells show strong EGFP expression. Photoreceptors have not generated OS at this developmental stage and express the rhodopsin-EGFP fusion protein in the entire cell. After maturation (a retinal section at PN29 is shown) rhodopsin expression and thus EGFP-positivity is restricted to the OS of photoreceptors whereas red fluorescence can be detected in all retinal cell types, including endothelial cells albeit in highly variable intensities (B). Cells of a dissociated PN4 rhoEGFP/DsRed retina after 4 days in culture. All cells show red fluorescence (DsRed), whereas many additionally express EGFP indicating them as rod photoreceptors (C). GCL, ganglion cell layer; INL, inner nuclear layer; IPL, inner plexiform layer; NB, neuroblast layer; ONL, outer nuclear layer; OS, outer segment. Scale bar: (A, B) 50 μm; (C) 20 μm. Adapted from Eberle et al., 2011.

After CD73-based MACS unsorted, negative and positive cell fractions were transplanted into the sub-retinal space of adult wild-type mice. Three weeks after transplantation, experimental retinas were analyzed for the integration of donor cells by fluorescence microscopy. Several DsRed-positive donor cells were found correctly integrated into the ONL of host retinas resembling the morphology of mature photoreceptors: a round, condensed nucleus containing a cell body located in the ONL, a synaptic terminal placed in the OPL, and an inner segment above the ONL (Figs. 9A–D). Furthermore, several integrated donor cells generated an EGFP-positive OS (Figs. 9A–D). Besides showing the characteristic morphology of mature photoreceptors and expression of rhodopsin-fused EGFP, all integrated donor cells expressed recoverin (data not shown; see also [16]). Quantification of integrated donor photoreceptors revealed a significantly higher integration rate of cells from the CD73-positive sorted fractions in comparison to negative or unsorted fractions. Whereas transplantation of unsorted or CD73-negative cells resulted in integration of 680 ± 410 cells/retina or 144 ± 102 cells/retina, respectively, CD73-positive cells showed an integration rate of 2199 ± 1006 cells/retina (Fig. 9E). Thus, the number of donor-derived photoreceptors that integrated into the ONL of adult hosts was increased by approximately threefold. We also found few integrated rhoEGFP-positive cells after transplantation of CD73-negative fractions. Beside some cells that may have escaped the sorting process, these cells may have been also originated from early photoreceptor precursors that had not developed further than the Crx or Nrl state and thus were CD73-negative when sorted (see the Discussion section).

Summing up, these data demonstrates, that MACS based on CD73 antibodies is a reliable method for the enrichment of transplantable photoreceptors resulting in an increased number of donor photoreceptors that successfully integrate into the adult mouse retina.

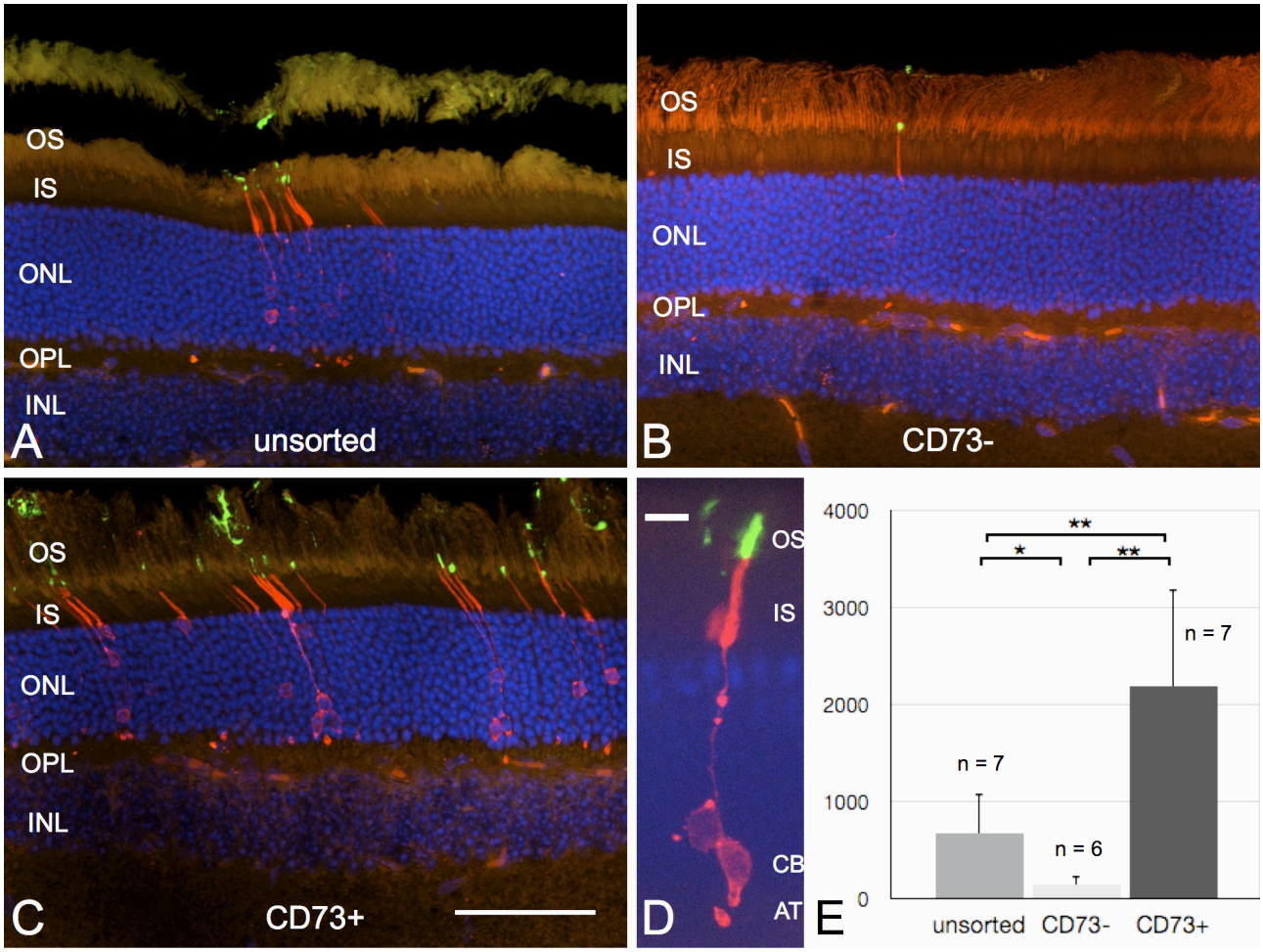

Figure 9: Integration of MACS-isolated donor cells into adult retinas. The integration potential of unsorted, CD73-negative, and CD73-positive retinal cells isolated from rhoEGFP/DsRed mice at PN4 was analyzed after transplantation into the sub-retinal space of adult wild-type mice. Donor cells identified by their expression of DsRed integrated into the ONL of hosts and developed the typical morphology of mature photoreceptors, including a round cell body (D, CB) located in the ONL, an axonal terminal (D, AT) in the OPL, and an inner segment (IS) above the ONL. In addition, most donor cells generated an OS identified by the distinct expression of GFP at the tip of the donor photoreceptors (A–C; a magnification of a donor photoreceptor is shown in D). Whereas the integration rate of CD73-negative cells was low (144 ± 102 cells/ retina; B, E), many cells from unsorted fractions were found in the ONL (680 ± 410 cells/retina; A, E). Transplantation of CD73-positive cell fractions significantly increased the number of integrated donor photoreceptors (2199 ± 1006 cells/retina; C, E). AT, axonal terminal; CB, cell body; INL, inner nuclear layer; IS, inner segment; OPL, outer plexiform layer; ONL, outer nuclear layer; OS, outer segment. *$P < 0.05$, **$P < 0.01$. Scale bar: (A–C) 50 μm; in (D) 10 μm. Adapted from Eberle et al., 2011.

2.3) Discussion

To date, there is no treatment available to regain visual function after degeneration of photoreceptor cells besides approaches using artificial retinal protheses [34]. Recent advantages in cell transplantation strategies for the replacement of photoreceptors in inherited forms of retinal degeneration have encouraged further research to pave the way toward clinical applications [15-17]. These preclinical studies provide evidence that pre-differentiated photoreceptors rather than stem and/or progenitor cells resemble a suitable cell type that has the potential to integrate into the adult mammalian retina and generate mature photoreceptors. Interestingly, initial data imply that donor-derived photoreceptors form functional connections to the endogenous neural circuitry [15,18]. One of the problems that limit a possible therapeutic use in patients is the low integration rate of transplanted cells into the ONL of hosts. Some improvements for donor cell integration were recently shown including short time disruption of the outer limiting membrane [20,21] and transplantation of purified cell suspensions enriched for photoreceptor precursors [17]. However, photoreceptor enrichment in the latter study was achieved by flow cytometry using reporter mice expressing GFP under control of the Crx promoter. Such genetic manipulation of cells before transplantation might impede their use in clinical applications.

In this study, we showed that cells within the rod photoreceptor lineage can be efficiently purified by MACS with antibodies against the cell surface molecule CD73. Enriched CD73- positive cell fractions contained ~87% rod photoreceptors (i.e., Nrl-EGFP-positive cells), an increase of approximately 40% the amount found in unsorted fractions. Indeed, microarray analysis demonstrated a more than threefold up-regulation of CD73 transcripts in rod photoreceptors in comparison to other retinal cells including retinal progenitors. These data confirm the recent findings [28] that CD73 is a reliable marker for photoreceptors in the mouse retina. Of note, CD73 is also a marker of rod photoreceptors in primates, as demonstrated in FACS-purified cells from the common marmoset retina

[28] implying that CD73 is a promising candidate for the enrichment of rods from human cell sources.

Notably, CD73-enriched cell fractions showed a significantly increased integration potential in comparison to unsorted cells after transplantation into adult mouse retinas. This finding demonstrates that purification of the proper cell type before transplantation is highly important and that young photoreceptors rather than retinal progenitors, which are mainly contained in the CD73-negative fractions, have the potential to integrate into the ONL. For transplantation, I used photoreceptors from double reporter mice that express DsRed ubiquitously as well as rhodopsin-EGFP fusion protein located on mature photoreceptor OSs, resulting in the identification of integrated donor cells without further staining procedures. Furthermore, rhodopsin-fused EGFP allows, for the first time, direct identification of fully mature photoreceptors and the detailed analysis of OS formation down to the ultrastructural level in wild-type mice, as well as mouse models of retinal degeneration after transplantation (see this work, section 3).

Technically, the use of cell surface antigens for the purification of young photoreceptors allows the separation of target cells by MACS. Compared to flow cytometry, the former method has the advantage that much more cells can be purified in a shorter period leading to increased photoreceptor survival. Indeed, I demonstrate here that the time-consuming sorting procedure to enrich a high number of photoreceptor precursors (e.g., by flow cytometry), results in increased cell damage and eventually death, which obviously negatively affects the survival rate of photoreceptor donor cells after transplantation [25]. However, flow cytometry has numerous advantages, including enrichment with highest purity and the possibility of separating cells by using multiple markers simultaneously. This process may also be necessary for optimizing sorts when specific sub-populations and/or additional combination with vital dyes are needed.

Therefore, reducing the procedure time may result at the end in an increase of integration rate as recently suggested [17].

In our hands, MACS resulted in an average enrichment of rod photoreceptors (Nrl-EGFP-positive cells) to 87% in CD73-positive fractions. Possibly the enrichment of rod photoreceptors by CD73 (the maximum in this study was 92.5% rods) can be further increased, for example, by optimizing the procedure, by direct coupling of paramagnetic micro-beads to the primary antibody, multiple sortings, prior negative sorting with cell surface antigens not expressed in photoreceptors, or controlling flow-through rates by the use of automated systems. There was no significant difference between the number of CD73-positive and Nrl-EGFP-positive cells in unsorted or CD73-positive fractions. Thus, rod photoreceptors represent the major CD73 expressing cell population in the retina. Furthermore, the number of rhoEGFP-positive cells was slightly but significantly reduced to Nrl-EGFP-positive cells in unsorted and CD73-positive cell fractions. In line with these findings, the number of rhoEGFP-negative cells was significantly higher than the Nrl-EGFP-negative cells in CD73-positive fractions. During photoreceptor development, Nrl precedes rhodopsin expression, and consequently our findings suggest that CD73 expression parallels that of Nrl and occurs before that of rhodopsin. Many of the rhoEGFP-negative cells in CD73-positive sorted cells may represent photoreceptor precursors at an earlier developmental stage that already express Nrl, but not rhodopsin. These results are in line with the hypothesis that the CD73 expression is downstream of Crx, upstream or parallel to Nrl, and upstream of rhodopsin in the developmental hierarchy of photoreceptors [28].

The purification of transplantable photoreceptors is of specific interest in light of recent advances in the generation of photoreceptors from pluripotent stem cell sources like ES or iPS cells [18,24-27]. Although very promising, the proportion of cells of the photoreceptor lineage generated from such cultures is still relatively low, thus requiring

effective sorting procedures before transplantation. Easy and fast separation methods like MACS, based on cell surface antigens, may be useful tools in this respect. However, the use of antibodies against solely CD73 may not represent the optimal sorting strategy since this antigen is not restricted to photoreceptors but could also be detected in other cell types—for example, T- and B-cell subsets and endothelial cells of capillaries and venules [35,36]. This wider expression profile may somehow impair the specific CD73 enrichment of photoreceptors from heterogenous cell cultures like those differentiating from pluripotent stem cells. Furthermore, during photoreceptor development CD73 expression follows up-regulation of Crx and then stays stable until photoreceptor maturation [28]. Thus, early (e.g., Crx-positive) photoreceptor precursors that might have integration potential after transplantation [17] are not included in the sorted cell fraction. In addition, more mature photoreceptors that might have limited integration capacity [15] can still be present after enrichment. This might avert a higher integration rate of sorted cells. As a consequence, new cell surface antigens that specifically recognize photoreceptors at a developmental stage that represents the ideal characteristics for integration have to be identified and evaluated. Furthermore, identification of cell surface markers for the exclusive separation of rods or cones may be an essential prerequisite for the development of cell-based therapies for retinal degenerative diseases characterized by either rod, as in RP, or cone, as in AMD, loss.

This study demonstrates that the enrichment of photoreceptor precursors from the neonatal mouse retina lead to increased integration into adult hosts. However, the absolute number of integrated donor photoreceptors remains relatively low (up to 3400 cells). In comparison to other published reports, it is obvious that the variability of successful cell integration is relatively high between studies and even within the same study ([15-17,20,22,29] and this study). Such variability may be due to diverse procedures and/or the techniques used, including cell dissociation, transplantation techniques, cell

reflux, genetic background, and age of donor and host mice, transgene reporters, and number of transplanted cells. However, enrichment of young photoreceptors could significantly increase the number of integrated cells ([17,29] and this study). Lakowski and colleagues reported 2010 integration numbers of 5,610 (median, range 754-15,402) cells / wt retina, using fluorescence-based sorting of Crx-GFP cells [17]. One year later, in 2011, they reported integration numbers of 13,134 (median, range 2,840-31,894) cells / wt retina using CD73-sorted Nrl-GFP cells [29], confirming our results of significant improvement of integration numbers using CD73-based cell surface antigen selection. Latest results by Pearson and colleagues indicate 16,759 ± 1,705 cells / wt retina using optimized transplantation procedures and 18,300 ± 1,474 cells per Gnat1-/- retina, a mouse model with no rod function but also no retinal degeneration [19].

In conclusion, the optimization and standardization of the entire transplantation process is of prime importance in bringing photoreceptor replacement closer to a clinical application, keeping in mind that the combined data reveal that the integration of a couple of thousand donor photoreceptors after transplantation into mouse models of retinal degeneration is still inefficient to cause functional changes that can be measured by electroretinogram ([17] and Ader M, unpublished data, 2010). Indeed, Pearson and colleagues reported recently, that 150,000 but not 60,000 rods are sufficient to elicit a reliable scotopic ERG response in Gnat1-/- mice [19]. Additionally, they reported a functional response in treated Gnat1-/- mice using a new water-maze setup, indicating that ERG measurements might be not sensitive enough to detect the currently small beneficial effects of PPC transplantation. In future, the purification of transplantable photoreceptors might be combined with methods that allow higher integration rates. For instance, these might include manipulation of the host tissue by acutely disrupting the outer limiting membrane using RNA interference technology [20,21], immune modulation [22,37], or co-injection of factors, allowing increased donor [38] cell migration and synapse formation like

MMP-2 or chondroitinase ABC [37,39]. Furthermore, it may be important to increase survival rates of transplanted photoreceptors [23,40] or implant donor cells into the sub-retinal space in a more oriented fashion instead of cell suspensions [41].

In conclusion, these results demonstrate the efficient enrichment of transplantable photoreceptors from the developmental mouse retina using cell surface-specific antibodies. Enriched cell fractions integrated with a significantly higher number into the ONL of adult hosts, generating mature, OS-forming photoreceptors. Thus, cell surface antigen-based enrichment of young photoreceptors represents a new and reliable method for cell transplantation studies to treat retinal degeneration characterized by photoreceptor cell loss.

3) Cell therapy: Outer segment formation of transplanted photoreceptor precursor cells

3.1) Introduction

While in the first part of this work, a quantitative enhancement of the integration capacity of transplanted photoreceptor precursor cells (PPCs) is investigated, the second part addresses the question of the quality of transplanted and integrated PPCs.

In preclinical studies it was demonstrated that donor PPCs isolated directly from the neonatal mouse retina at postnatal day (PN) 3-5 have the highest potential to develop into mature photoreceptors [15-17,29], which form axonal terminals and inner (IS) and outer (OS) segments [30] following grafting into the retina of adult hosts. While a properly developed OS with well-aligned disc membrane staples is crucial for light detection and conversion into an electric signal, an axonal terminal that connects to the respective bipolar cell is indispensable for transmitting the electric signal to the host neural circuitry. Functional analyses, such as electroretinogram (ERG) recordings, pupillary reflexes, opto-kinetic tracking or visual Morris water maze, have been described after transplantation of PPCs into murine models of retinal degeneration (RD) suggesting improvements in visual function [15,18,19,25,42]. Nevertheless, these studies still lack the direct morphological evidence for proper OS formation.

Pioneer studies by Gouras et al. [11,43,44] and Bartsch et al. [16] suggesting OS formation of transplanted photoreceptors were impeded due to the lack of optimal labeling methods of donor OSs. Similarly, all other studies on photoreceptor transplantation failed as well to demonstrate formation of OS due to the absence of fluorescent reporter proteins in the OS of transplanted PPCs [15-17,19,29]. Here, I took advantage of a recently generated transgenic reporter mouse line in which enhanced green fluorescent protein (EGFP) is fused to human rhodopsin protein, the main photopigment in rod photoreceptors

[33], to investigate these issues. Rhodopsin is exclusively located to the OS of mature rod photoreceptors allowing detailed ultra-structural analysis of their formation and integrity upon the transplantation of PPCs into adult mouse retinas. Using such model organisms combined with the isolation of PPCs based on CD73 as a cell surface marker I successfully demonstrate that transplanted PPCs are able to form a native OS including the formation of a connecting cilium and well-aligned disc membrane staples, the latter structure being an indispensable morphological prerequisite for proper light detection. Remarkably, the OS formation was not restricted to transplanted cells correctly integrated into the ONL but was also observed when photoreceptors remained in the sub-retinal space of the host.

3.2) Results

3.2.1) Visualization of outer segments using fluorescence light and electron microscopy

Correlative light and electron microscopy (CLEM) investigations were performed in collaboration with Thomas Kurth and Susanne Kretschmar from the electron microscopy facility, CRTD, TU Dresden.

CLEM combines fluorescent light microscopic (FLM) labeling with electron microscopy (EM), enabling studies of bulky tissue samples from low to sub-cellular high resolution [45-47]. We took advantage of the CLEM flexibility to localize the rare events of PPC integration, and to study the formation of OS at an ultra-structural resolution.

To demonstrate the feasibility of immuno-CLEM on retina samples as a proof of principle, adult eyes from a rhoEGFP mouse were isolated, embedded in Lowicryl K4M resin, and ultra-thin sections were immuno-labeled using anti-GFP antibodies (Fig. 10). The rhoEGFP transgenic animals were characterized by the expression of EGFP fused to human rhodopsin [33], which is exclusively located in the photoreceptor OS (Fig. 10A). As expected, a strong overlapping signal of rhoEGFP per se and the immuno-labeling (Fig. 10B) was observed exclusively within OSs (Fig. 10C). At transmission electron microscope (TEM) level, sections derived from the same block labeled with anti-GFP antibodies followed by protein A 10-nm gold revealed that immuno-labeling is specific for photoreceptor OSs demonstrating that these light detecting structures can be visualized at an ultra-structural resolution based on a targeted EGFP expression (Fig. 10D, D').

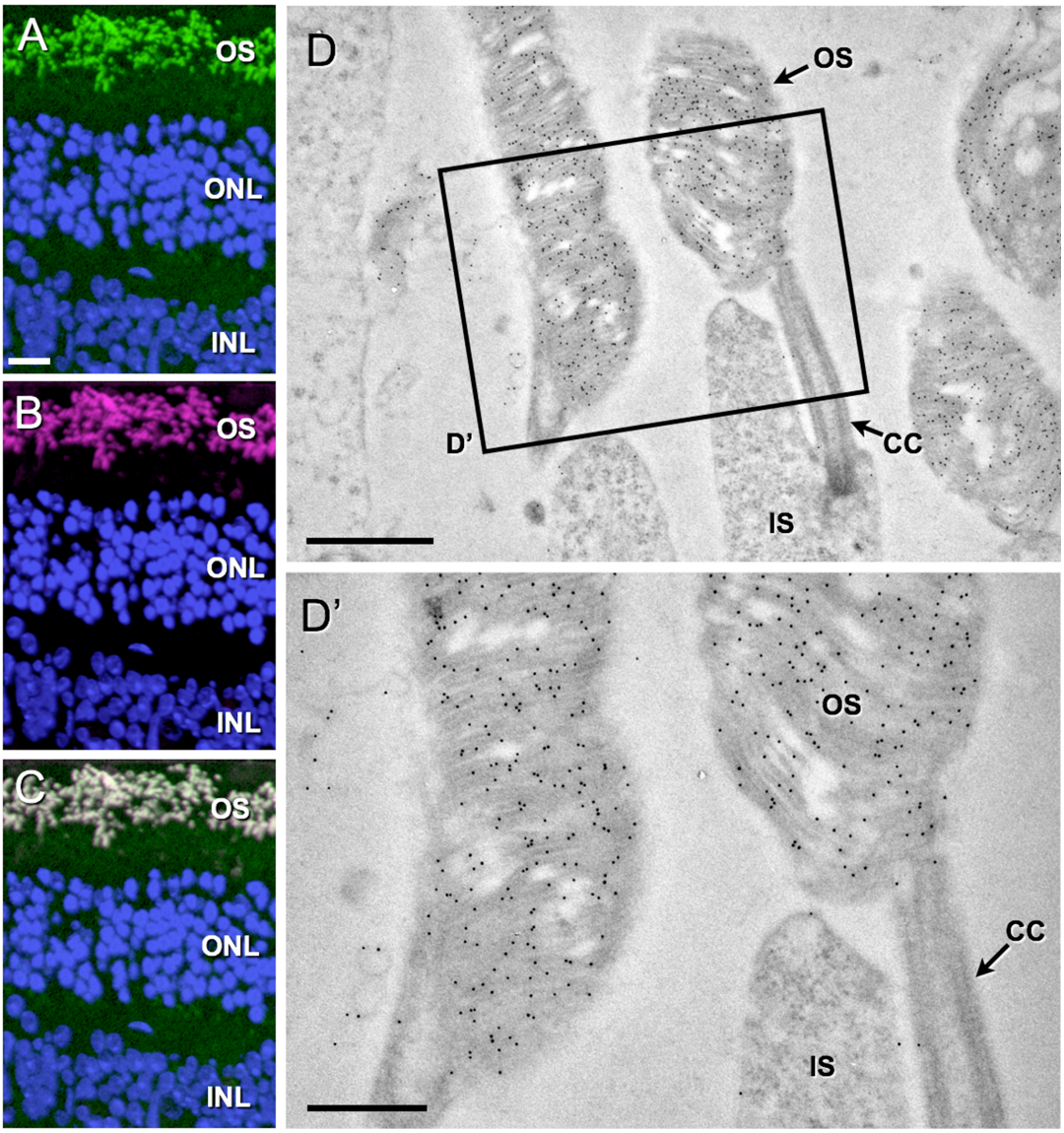

Figure 10: Ultra-structural identification of outer segments from rhoEGFP transgenic mice. The 200-nm thin K4M-resin sections of a retina isolated from an adult rhoEGFP mouse were immuno-stained with anti-EGFP antibodies followed by goat anti-rabbit Alexa555 (A-C). RhoEGFP fluorescence (A, green) is restricted to the outer segments (OS) of photoreceptors and completely overlaps with the immuno-fluorescent signal (B, magenta; C is the merged image of A and B). Outer (ONL) and inner (INL) nuclear layers are highlighted by DAPI staining (blue). For ultra-structural analysis, resin sections from a rhoEGFP retina were immuno-stained with anti-EGFP antibodies, followed by protein A 10-nm gold (D; D' is a high power image of the boxed region in D). Note the specific immuno-labeling of OSs containing the typical disc membrane staples characteristic for mature photoreceptors. CC, connecting cilium; IS, inner segment. Scale bars: A-C: 20 μm, D: 1 μm, D': 500 nm. Adapted from Eberle et al., 2012.

3.2.2) Transplanted photoreceptor precursor cells integrate into wild-type host retinas and form native outer segments with well-aligned disc membranes

To demonstrate whether PPCs transplanted into a wild-type (wt) retina develop proper OSs, I used a dual strategy based on one hand on their paramagnetic immuno-isolation by means of CD73 as a selective cell surface marker [30], and on the other hand on double-(actinDsRed, rhoEGFP) transgenic reporter animals, which allow to visualize the transplanted cells in the host wt retina. Indeed, the actin-driven DsRed expression highlights the entire cell body of transplanted PPCs with exception of the OS that is labeled by EGFP (i.e. rhoEGFP, see above). Donor PPCs were isolated from postnatal day (PN) 4 animals for all experiments in this study.

Three weeks post-transplantation, a sub-fraction of transplanted PPCs successfully integrated into the ONL of wt mice with an integration rate similar to our previous investigations, i.e. about 2000 ± 1000 cells/retina [30]. Donor cells showed DsRed-expression in the whole cell body including the axonal terminal connection within the outer plexiform layer (OPL) (Fig. 11A, white), while rhoEGFP-expression was detectable exclusively in elongated, tubular structures of approximately 5-15 μm length and 1 μm width apical to the rest of the cell body (Fig. 11A, green). Since the latter structure has the typical shape and localization of a photoreceptor OS, it is highly probable that transplanted PPCs develop an OS, too. CLEM analysis of single ultra-thin sections mounted to finder grids (Fig. 11B) revealed rhoEGFP–positive elongated tubular structures (Fig. 11B': boxed area in B; Fig. 11C, C', arrow).

At high-resolution level, these fluorescent structures (e.g. see Fig, 11D', arrow) turned out to be morphologically normal OSs (Fig. 11D, TEM-micrograph corresponding to FLM image in D'). Thus, OSs of the transplanted cells displayed well-aligned disc membranes growing out from a connecting cilium (Fig. 11E-E"). Although the overall membranous organization of the vast majority (20 out of 21) of analyzed transplanted

rhoEGFP–positive photoreceptor OSs was indistinguishable to that of native photoreceptor cells found in the host retina (Fig. 11F), we observed in few cases donor cells harboring slight disturbances of the alignment of disc membranes within OSs (data not shown). Such phenomena might be the result of the sample preparation or might represent individual cellular variances, since they were also observed in rare cases in host photoreceptor OSs.

Technically, it is important to point out that a careful observation and interpretation of fluorescent OSs are crucial since certain unidentified auto-fluorescent structures in the area of host OSs (Fig. 11B', C, arrowhead), might correspond to false–positive signals as detected by TEM (Fig. 11C'). Taken together, we demonstrated technically a powerful method to analyze the ultra-structure of the OSs of transplanted PPCs into host retinas, and revealed from a cell biological point of view that PPCs integrated into the host ONL are able to develop morphologically normal OSs.

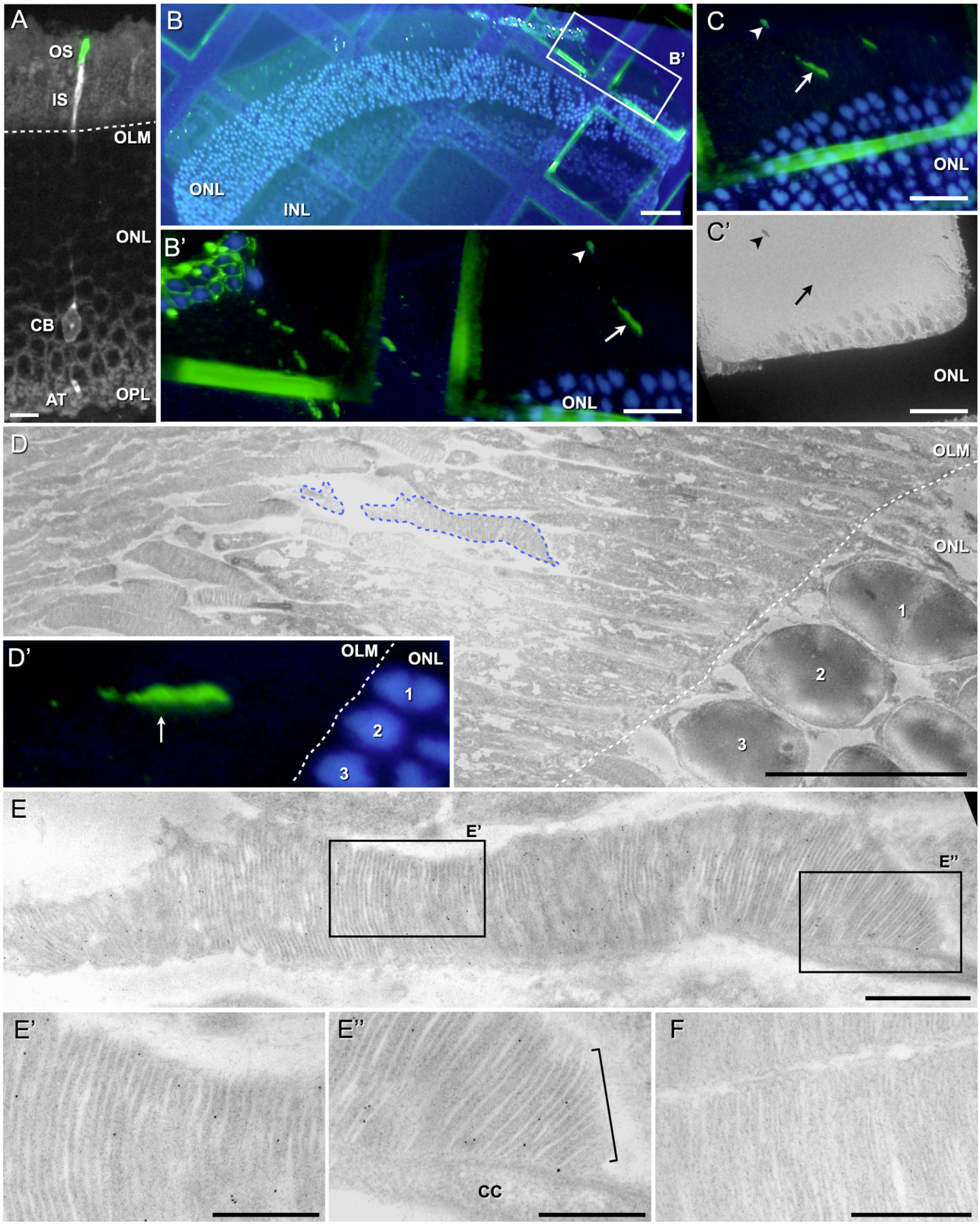

Figure 11: Integrated donor rhoEGFP–positive photoreceptors generate outer segments in wild-type host retinas.

Figure 11: Integrated donor rhoEGFP–positive photoreceptors generate outer segments in wild-type host retinas. Upon transplantation into an adult wild-type mouse (A), CD73-enriched photoreceptor precursor cells (PPC) isolated from double-transgenic (rhoEGFP, actinDsRed) reporter animals integrated properly into the host retina and developed the typical morphology of mature photoreceptors, including a round cell body (CB, white) located in the outer nuclear layer (ONL), an axonal terminal (AT) in the outer plexiform layer (OPL) as well as an inner (IS, white) and outer (OS, green) segment located above the outer limiting membrane (OLM, dashed line). On a representative correlative light electron microscopy section (B; B' is a higher power view of the boxed area in B) rhoEGFP–positive elongated structures could be observed (B', arrow). Cell nuclei are stained with DAPI (blue). Note that not every green fluorescent signal in the area of host OSs indicated the presence of biological structures since unspecific signals (B', C and C', arrowhead) could mimic the typical ones of a rhoEGFP–positive OS (C, arrow), which was not observable in low-magnification transmission electron microscopy (TEM) in contrast to the contamination (C', arrow and arrowhead, respectively). RhoEGFP–positive OSs derived from integrated, transplanted PPCs showed the physiological elongated morphology as observed by TEM (D, blue dashed line; E) and the corresponding fluorescent light microscopy image (D', arrow; as reference points three nuclei were numbered). The boxed areas in E are shown at higher magnification in the respective panels E' and E". Note that in addition to the formation of a connecting cilium (E", CC) the donor-derived OSs displayed growing membrane evaginations at their bases (E", bracket) and typical densely packed disc membrane staples (E', E") similar to endogenous OSs (F). Scale bars: A: 10 μm, B: 50 μm, B'-C': 20 μm, D: 10 μm, E: 1 μm, E'-F: 500 nm. Adapted from Eberle et al., 2012.

3.2.3) Non-integrated cells in the wild-type sub-retinal space develop an outer segment

Several studies suggest that transplanted photoreceptors form OSs when integrating into the ONL of experimental animals [15,16,19,30,43,44]. However, patients with severe RD are characterized by an almost absence of photoreceptor cells and are thus missing a proper ONL structure that would allow integration of donor cells. Indeed, the integration rate of transplanted PPCs strongly decreases in mouse models of RD characterized by a severe loss of the ONL ([48,49] and see below) and non-integrated donor photoreceptors fail to form the typical elongated morphology of mature wt photoreceptors. Also, following transplantation into a normal environment, the majority of grafted photoreceptors remains in the sub-retinal space and does not develop photoreceptor morphology [16].

Using CD73-enriched donor cells isolated from double-(actinDsRed, rhoEGFP) transgenic reporter mice I observed that transplanted cells located in the sub-retinal space of wt hosts do not develop the elongated morphology of integrated photoreceptors as seen in Figure 11A. In contrast, I observed round DsRed–positive cell bodies with adjacent longitudinal, EGFP–positive, OS-like structures (Fig. 12A, arrows). Ultra-structural analysis revealed that EGFP–positive extensions were native-like OSs containing well-aligned disc membrane staples (Fig. 12B-B”) in the majority of studied OSs (35 out of 40). Therefore, I conclude that donor photoreceptors not only form native-like OSs when correctly integrating into the ONL of the host but also when remaining in the sub-retinal space.

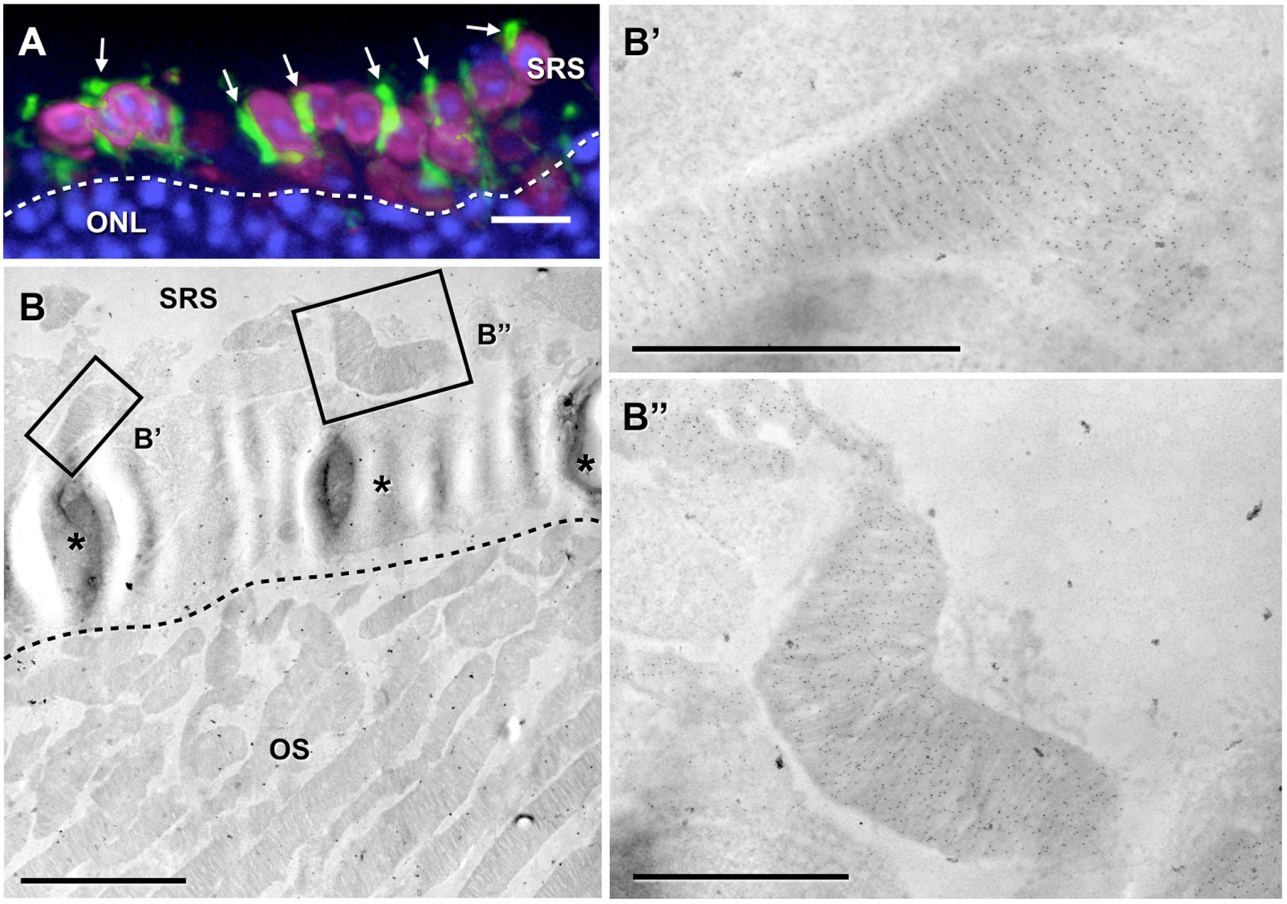

Figure 12: Transplanted photoreceptors remaining in the sub-retinal space generate outer segments. Upon transplantation into an adult wild-type mouse (A), many CD73-enriched photoreceptor precursor cells (PPC) isolated from double-transgenic (rhoEGFP, actinDsRed) reporter animals remain in the sub-retinal space (SRS) at the top of the host outer nuclear layer (ONL, dashed line) and develop outer segment (OS)-like structures that are labeled with rhoEGFP (green, arrows). The cell body of transplanted cells is observed by DsRed-expression (magenta) whereas cell nuclei are stained with DAPI (blue). An electron microscopy overview (B) of transplanted PPCs found in the SRS demonstrates that several of them (asterisks) lay above the host photoreceptor OSs, which are delimitated by a dashed line. Magnifications of the boxed areas in panel B reveal that the non-integrated PPCs developed as well organized disc membrane staples, which are positive for rhoEGFP (B’, B”, black dots). Scale bars: A: 10 μm, B: 5 μm, B’ and B”: 2 μm. Adapted from Eberle et al., 2012.

3.2.4) Transplanted photoreceptor precursor cells do not integrate in P347S host retinas but form outer segments in the sub-retinal space

In the previous sections we have shown that PPCs have the potential to form OSs when integrated into the ONL or remaining in the sub-retinal space of wt hosts. Based on these results, I further investigated whether a similar phenomenon might occur in severely degenerated retinas. P347S transgenic mice represent a valuable model for autosomal-dominant retinal degeneration, and heterozygous animals loose the majority of photoreceptors within 12 weeks ([50], our unpublished observations).

Following transplantation of CD73-enriched PPCs derived from double-(actinDsRed, rhoEGFP) transgenic mice into heterozygous P347S mouse retinas (4 and 12 weeks old), I observed the formation of cell clusters located in the sub-retinal space (Fig. 13A). Integration of grafted cells into the remaining ONL, which consists solely of 1 or 2 nuclei thickness in 12 weeks old mice, was not observed three weeks post-transplantation (Fig. 13A). Nevertheless, the majority of donor photoreceptors had formed longitudinal, rhoEGFP–positive OS-like structures next to their DsRed-positive cell bodies (Fig. 13A‘) as observed above upon transplantation in healthy animals. We could not observe a consistent OS polarity, neither towards the RPE nor the ONL, of sub-retinal located donor cells in wt as well as in p347s animals. Electron-microscopic analysis revealed the formation of OSs with well-aligned disc membranes (in 8 out of 16 examined sub-retinal OSs), demonstrating the potential of transplanted PPCs to form native OS structures in a heavily degenerated retina, and this without cellular integration into the host tissues (Fig. 13A“, A“‘).

To evaluate if such sub-retinal located donor photoreceptors are light-sensitive we analyzed the sub-cellular localization of transducin, a molecule of the light transduction pathway that is present in the OS in the dark and translocates to the inner segment/cell body upon light stimulation. Indeed immuno-histochemical analysis showed that transducin

is predominantly present in OSs of donor photoreceptors in dark-adapted mice (Fig. 13C - C'") whereas in light-adapted mice, it could only be detected in the cell body (Fig. 13B – B'"). Furthermore, as rhodopsin represents the first protein in the light transduction pathway and has to be highly expressed in functional photoreceptors, we analyzed the generation of rhodopsin by immuno-histochemistry to determine its expression at the protein level. Indeed, labeled donor photoreceptors showed similar fluorescence intensities as endogenous photoreceptors in all transplantation paradigms (Fig. 14).

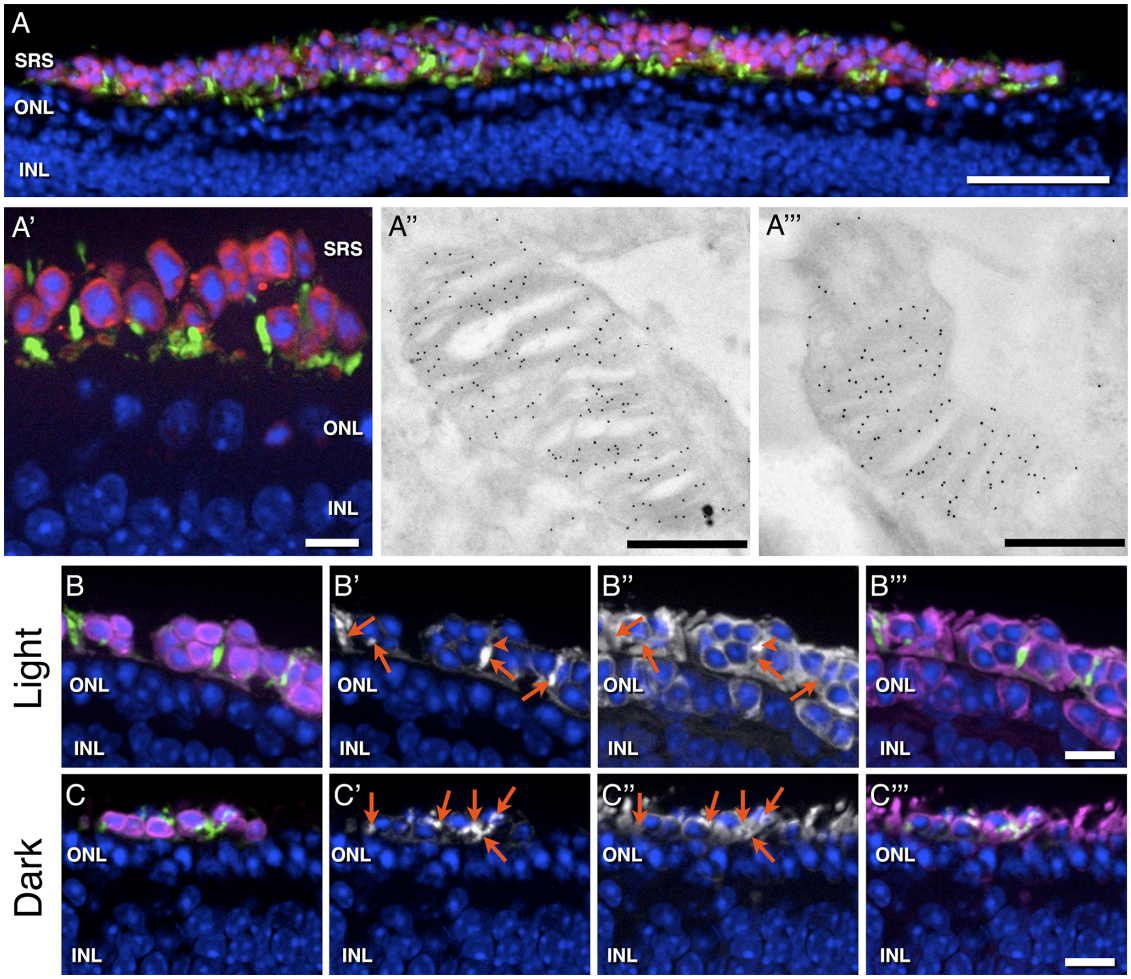

Figure 13: Transplantation of rhoEGFP–positive photoreceptors into the degenerated retina of heterozygous P347S mice. Low and high magnification views (A, A‘) of a degenerated retina from a heterozygous P347S mouse, 3 weeks post-transplantation of CD73-enriched photoreceptor precursor cells isolated from double-transgenic (rhoEGFP, actinDsRed) reporter animals. Cell nuclei are stained with DAPI (blue). Note, that transplanted cells (cell body, magenta; outer segment, green) are found in a sheet-like structure in the sub-retinal space (SRS), i.e. above the host outer nuclear layer (ONL), which is reduced to only 1 - 2 cell rows. Electron microscopy analyses of rhoEGFP–positive structures reveal the formation of ultra-structurally normal OSs containing morphologically native disc membrane staples (A'', A'''). In light adapted animals (B-B'''), transducin (B'', white and B''', magenta) is expressed in OSs of transplanted, sub-retinal PPCs at low levels (B' and B'', arrows), whereas high levels of transducin could be detected in IS-like structures next to rhoEGFP-positive OSs (B' and B'', arrowhead). In contrast, dark adapted animals show significantly higher levels of transducin in rhoEGFP-positive OSs (C' and C'', arrows), indicated also by white overlay staining in C'''. This illustrates, that sub-retinal PPCs show the native translocation of transducin under different light conditions, which is a prerequisite for functionality. INL, inner nuclear layer. Scale bars: A: 50 μm, A': 10 μm, A'', A''': 500 nm, B-B''' and C-C''': 10 μm. Adapted from Eberle et al., 2012.

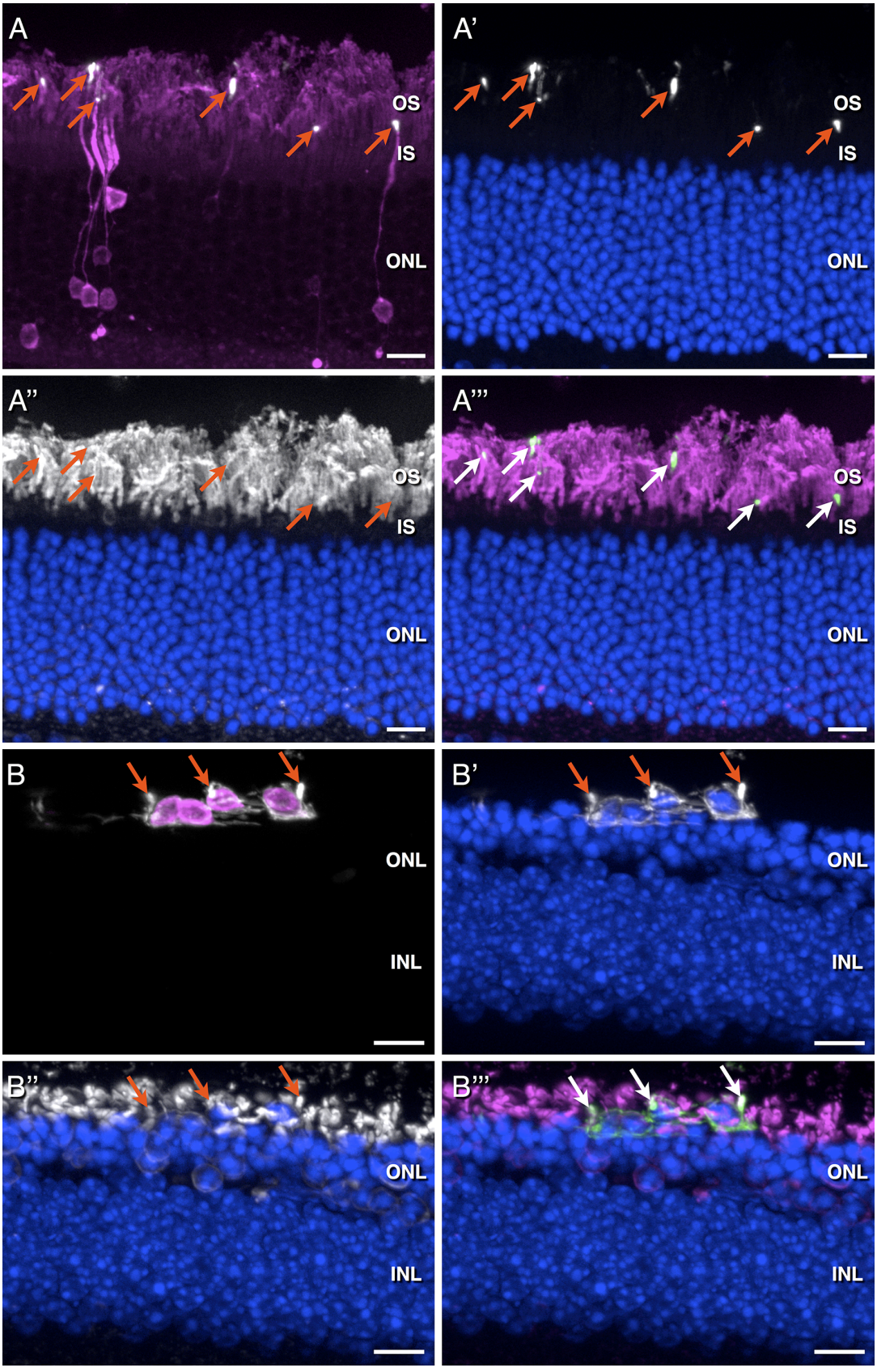

Figure 14: Rhodopsin expression in rhoEGFP-positive OSs.

Figure 14: Rhodopsin expression in rhoEGFP-positive OSs. Rhodopsin expression was detected in rhoEGFP-positive OSs of integrated donor cells in wt (A-A''') as well as in rhoEGFP-positive OSs of sub-retinal located cells in P347S mice (B-B'''). DsRed-positive, transplanted PPCs (A, magenta) show, following integration into the host wt ONL, typical green fluorescent, rhoEGFP-positive OSs at the tip of their ISs (A, A', white and A''', green) highlighted by arrows in A-A'''. Rhodopsin staining (A'', white and A''', magenta) reveals a relatively equal expression throughout the OSs of the wt host. The rhoEGFP-positive OSs co-localize with rhodopsin immuno-staining (compare A' and A'', arrows), indicated by white overlap staining in A''' (arrows). Following transplantation into P347S mice sub-retinal located DsRed-positive PPCs (B, magenta) develop the characteristic rhoEGFP-positive OSs adjacent to the cell body (B, B', white and B''', green). The rhoEGFP fluorescence co-localizes with rhodopsin staining (compare B' and B'', arrows), indicated by white overlap staining in B'''. Similar rhodopsin expression levels are detectable in host and donor cells (A, B) suggesting a native expression of rhodopsin in rhoEGFP-positive OSs of transplanted and integrated as well as sub-retinal located PPCs. Scale bars: 10 μm. Adapted from Eberle et al., 2012.

3.2.5) The sub-retinal space provides a supporting environment for outer segment generation of transplanted photoreceptor precursor cells

The data presented above demonstrate, that PPCs located to the sub-retinal space of both, wt and degenerated retinas, develop native-like OSs. This prompted me to investigate whether the OS formation by transplanted donor cells is a cell autonomous property or depends on environmental factors. To address this issue, I injected simultaneously donor PPCs into the sub-retinal space and the vitreous side of four-weeks old P347S transgenic hosts (Fig. 15).

As shown above, PPCs located in the sub-retinal space developed the typical OS-like structures with high-levels of rhoEGFP expression (Fig 15A, A'). In sharp contrast, when transplanted to the vitreous side, donor cells expressed significant lower amounts of rhoEGFP (Fig. 15A). Indeed, EGFP-positivity of vitreal located donor PPCs could only be visualized by increasing the saturation level of the green fluorescence channel of the same image (Fig. 15B; B' is a higher magnification of the boxed area in B). Furthermore, FLM analyses suggested that in comparison to PPCs injected to the sub-retinal space (Fig. 15A'), the ones located on the vitreous side generated OS-like structures less frequently (Fig. 15B', arrows; ultra-structurally 7 out of 16 analyzed donor cells showed an OS-like structure) and that these were poorly developed (Fig. 15B'; see also Fig. 16A, B). CLEM analysis revealed that these structures are, in all cases (7 out of 7), altered OSs with abnormal arrangement including disorganized disc membrane staples (Fig. 16D, E). Occasionally, we observed a mis-localization of rhoEGFP to the plasma membrane of the soma (Fig. 16F). Taken together, these findings indicate that the sub-retinal space, in contrast to the vitreous one, supports the maturation of transplanted PPCs and proper biogenesis of OSs.

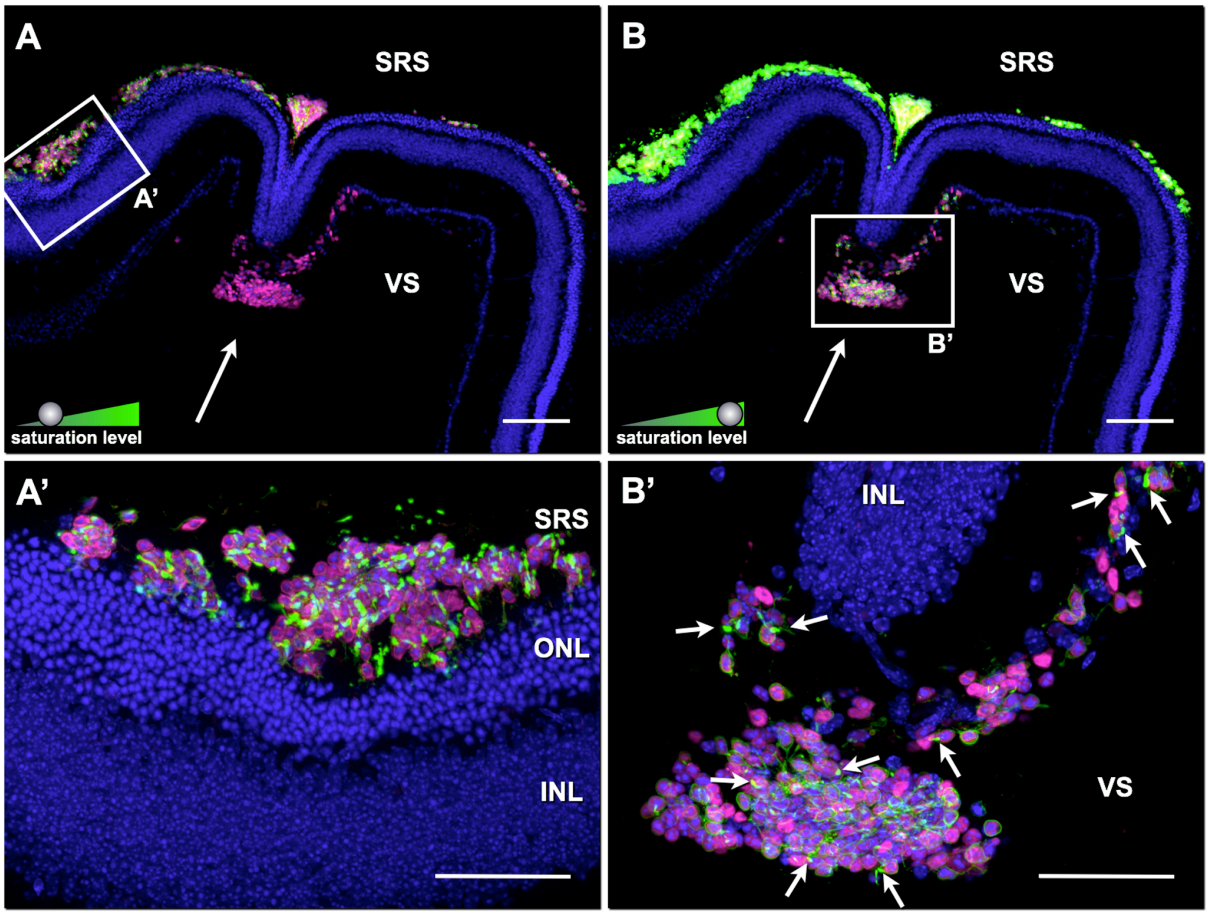

Figure 15: Differences in outer segment formation between sub-retinal and vitreal located transplanted photoreceptor precursor cells. CD73-enriched photoreceptor precursor cells (PPC) isolated from double-transgenic (rhoEGFP, actinDsRed) reporter animals were simultaneously transplanted into the sub-retinal (SRS) and vitreous (VS) space of 4-weeks old P347S hosts (A; B is the same image as A but with increased green fluorescence channel saturation level). Cell nuclei are highlighted with DAPI staining (blue). Donor cells (magenta) were detected in the SRS (e.g. boxed area in A) and VS (A and B, arrow) showing survival of transplanted cells in both locations. Whereas sub-retinally injected PPCs showed strong EGFP expression (green; e.g. boxed area in A), vitreally injected donor cells appeared almost devoid of EGFP signal (A, arrow). However, by increasing the saturation level of the green fluorescence signal channel in image A, faint EGFP signal could be detected in the vitreally located donor cells (B; B' is a separate image with adjusted shutter time showing a magnification of the boxed area in B) demonstrating that donor cells located in the SRS had higher rhoEGFP expression levels than those in the VS (compare different cell populations in each individual panel A and B). Moreover, almost every single sub-retinal located donor PPC showed rhoEGFP labeled OSs (A'), in contrast to those located in the VS that generated only in few cases OS-like protrusions (B', arrows). ONL, outer nuclear layer; INL, inner nuclear layer. Scale bars: 50 μm. Adapted from Eberle et al., 2012.

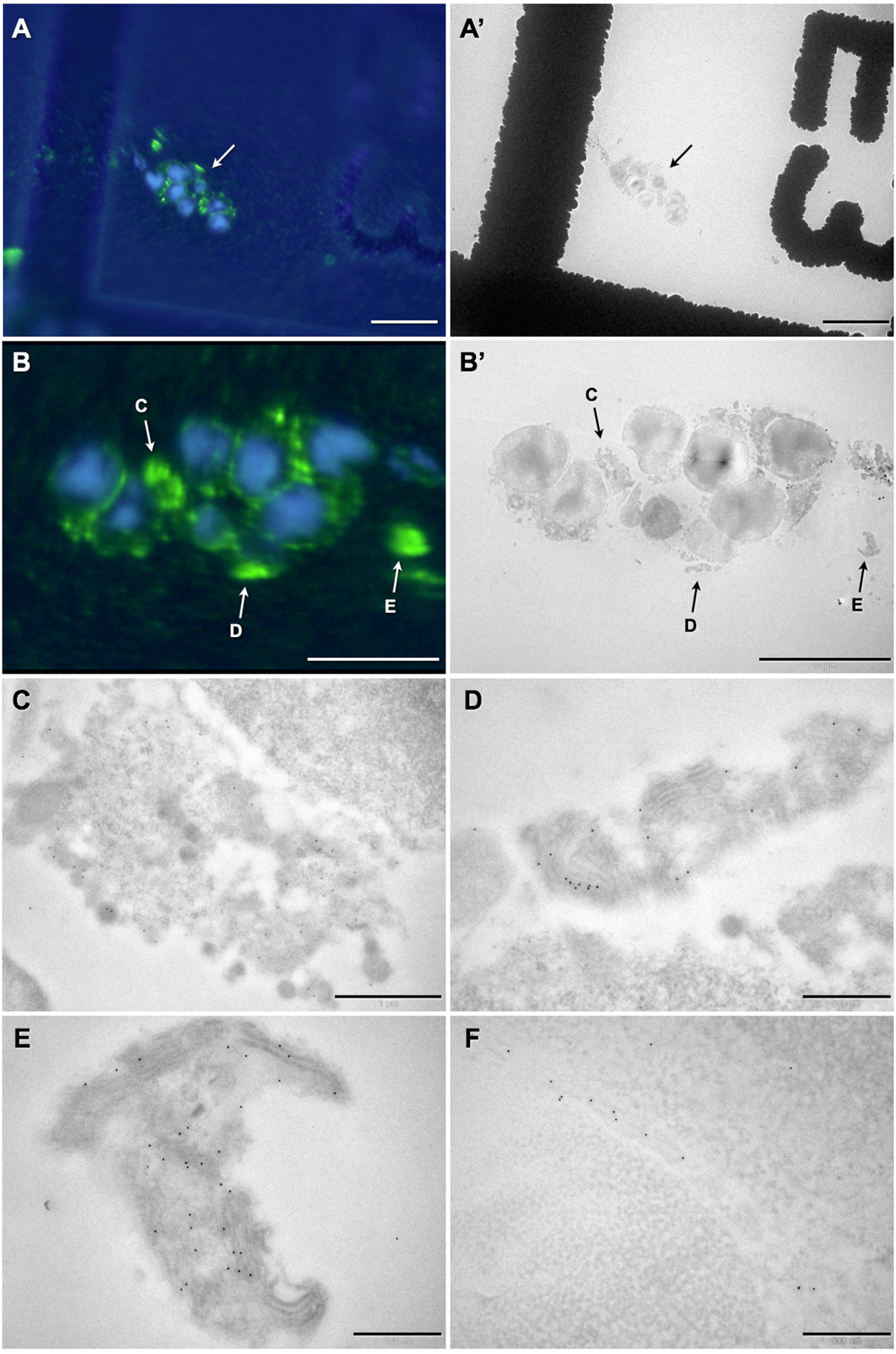

Figure 16: Vitreal-located transplanted photoreceptor precursor cells develop disturbed outer segment-like structures with misaligned disc membranes.

Figure 16: Vitreal-located transplanted photoreceptor precursor cells develop disturbed outer segment-like structures with misaligned disc membranes. CLEM analysis on resin sections allowed examination of vitreally-transplanted rhoEGFP–positive photoreceptor precursor cell aggregates. Cell nuclei are highlighted by DAPI staining (blue). A representative example is shown with fluorescence light microscopic- (A) and transmission electron microscopic-illumination (A'). The donor cells in A and A' are shown at higher magnification in the respective panels B and B'. RhoEGFP-enriched structures (A, B; green, arrows) next to the cell bodies suggest the formation of OSs, and three of these (C, D and E) are displayed in the corresponding panels at a high-resolution level by TEM-analysis. These structures appear either as rhoEGFP-enriched cell debris (C) or rhoEGFP–positive OS-like structures with an abnormal organization/ integrity including misaligned disc membranes (D, E). Additionally, mislocation of rhoEGFP to the plasma membrane of the soma was observed (F). Scale bars: A, A': 20 μm, B, B': 10 μm, C: 1 μm, D-F: 500 nm. Adapted from Eberle et al., 2012.

3.3) Discussion

In the present study, a unique system that combines the use of transgenic mouse lines and CLEM to analyze the peculiar morphological details of the OS structure of transplanted PPCs is reported. Three major cell biological observations were made using such bio-technical tools. First, we demonstrated that integrated PPCs develop into mature photoreceptor cells with appropriate OS structures. Second, we show that PPCs remaining in the sub-retinal space of wild-type as well as degenerated retinas generate also proper OSs and third, we revealed that environmental factors found in the sub-retinal space influence PPC differentiation and maturation.

PPCs have been studied as a possible therapeutic option for the replacement of lost photoreceptors in pre-clinical mouse models since their first successful transplantation already two decades ago [12,13,43,44]. Recent reports have revealed their ability to integrate and differentiate into mature photoreceptors when transplanted into host retinas [15,16,19]. Indeed, studies indicated that upon integration into the host ONL donor PPCs develop adequate axonal terminals containing ribbon synapses located in the OPL whereas their ISs and OSs lie in the photoreceptor layer just above the outer limiting membrane [15,16,30]. Direct evidence for proper OS formation was however impeded due to the lack of adequate transgenic animal models allowing the accurate tracking of transplanted cells [15,16,19,29]. For instance, most of the studies used soluble, cytoplasmic fluorescent reporter proteins, which in essence strongly limits their targeting towards the photoreceptor OS. Addressing the latter issue is particularly important given that the key feature of photoreceptors enabling correct light detection relies on the aligned disc membrane staples of their OS.

To settle such technical difficulty we used here transgenic animals as a source of donor cells where prospective OSs of transplanted cells could be visualized with a fluorescent reporter protein specifically targeted to the OSs by means of rhodopsin as a

carrier protein. By combining CLEM with indirect immuno-labeling of the reporter-fusion rhodopsin-EGFP protein we demonstrated that integrated donor PPCs develop OSs with proper morphological structures that included the formation of a connecting cilium followed by aligned disc membrane staples. Moreover, short membrane evaginations growing from the connecting cilium at the base of OSs are detectable, consistent with the normal biogenesis of these photoreceptive structures. In addition, our investigations reveal unexpectedly that transplanted PPCs, which are not integrated into the host ONL, but remained in the sub-retinal space, generated also proper OSs. This observation is independent from the degenerative state of the host retina since a similar phenomenon was detected when PPCs were transplanted into severely degenerated retinas of P347S transgenic mice. Therefore, it appears that the formation of normal OSs from transplanted PPCs is independent of their integration into the ONL.

The cell biological properties of transplanted PPCs to form proper OSs independently of their integration within the host ONL may rely either on cell autonomous cues or cellular factors provided by the microenvironment found in the host retinas. To further dissect these possibilities, I have differentially transplanted the PPCs into the sub-retinal space and vitreous side. Interestingly, we found that PPCs transplanted into the vitreous side express significant lower amounts of rhodopsin-EGFP and develop aberrant OSs by comparison to those injected to the sub-retinal space. Such data suggest that the maturation of PPCs as monitored by the expression of rhodopsin and formation of OS are provided by factors found specifically in the sub-retinal space. One major cellular player that could explain such singularity is the retinal pigment epithelium (RPE) adjacent to the sub-retinal space. Indeed, RPE cells have been shown to promote photoreceptor cell development, survival, neurite outgrowth and differentiation [51-53] as well as OS development, maintenance and regeneration [54,55]. A direct connection of donor OSs with endogenous RPE cells does not seem to be necessary since OS formation is

observed throughout the sub-retinal PPC population even when forming multiple layers of cells. As a consequence, I propose that factors secreted from the RPE have an important influence on the stimulation of transplanted PPCs to mature and form OSs. However, a correct alignment and growth towards the RPE was not observed. We therefore conclude, that these factors stimulate maturation and formation of OSs but are not sufficient for their correct alignment. Since in eye development the outgrowing OSs are tightly packed next to each other, it might be important for future studies to provide a scaffold for correct alignment and targeting of OSs developed by sub-retinal located PPCs.

The findings of this study are of prime importance to further develop this promising treatment strategy towards clinical application. Indeed, photoreceptor cell-based replacement therapy is founded on three main pillars. First, it is indispensable to establish a reliable and continuous source for transplantable materials. Second, a transplantation method providing a significant number of integration events and long-term survival of donor cells is a technical pre-requisite, and third, maturation including OS formation and functional integration of donor PPCs into the neural circuitry of the host retina are a must. Several teams are currently investigating the potential of diverse *in vitro* expandable cell populations for the generation of transplantable photoreceptors. These cell sources include i) expandable cells isolated from the retina, the so-called “retinal stem cells” [56-59] and ii) pluripotent stem cells, i.e. embryonic stem cells (ESC) [18,24] and induced pluripotent (iPS) stem cells [25,42,60]. Whether such produced or manufactured donor photoreceptors have however the potential to generate proper OS structures following grafting as demonstrated here for PPCs remains to be evaluated. Obviously, the double-(actinDsRed, rhoEGFP) transgenic animals might be used as cellular sources to generate such *in vitro* expandable donor cells to solve such issues.

Finally, I have documented that PPCs transplanted to the sub-retinal space have the potential to form proper photoreceptor OSs even when they are not integrated into the

host ONL. A phenomenon observed as well in RD models (e.g. P347S: this work; rhodopsin knock-out: our unpublished observations). However, the lack of integration into the latter models raised some biomedical questions. Barber and colleagues have also linked a negative correlation between grade of degeneration and integrative potential into the host ONL in most retinal degeneration models studied [48,49]. Such issues are particularly important when we are thinking about patients at late stage RD, i.e. who are blind or close to blindness and show a strong, if not a total degenerated ONL. Although, it appears unlikely at first glance that transplanted PPCs will successfully integrate into degenerated retinas of such affected patients (this study and [48,49]), a recent study demonstrated that following transplantation into a slow degeneration mouse model of RP (i.e. Gnat1-/- mice), PPCs are able to integrate into the host ONL and functionally connect to the neural circuitry by forming active synapses with endogenous interneurons [19]. Together with our results demonstrating OS formation and light sensitivity of donor photoreceptors in strongly degenerated retinas without integration, such achievements indicate that visual improvement might also be possible in late stage retinal degenerations. However, detailed investigations of functional integration of donor cells into the host neural circuitry at the cellular and behavioral level still have to be performed to evaluate the potential of transplanted photoreceptors in the heavily degenerated retina. Collectively, these findings represent a major step on the way towards the development of a cell-based replacement therapy of diseases characterized by photoreceptor loss.

4) Gene therapy: Rescue of prominin-1 knock-out mouse phenotype by introducing wild-type prominin-1 using rAAV vectors

4.1) Introduction

After qualitative and quantitative investigations for a cell therapy, the third part of this work addresses a gene therapeutical approach for retinal degenerative disorders.

To date, mutations in 69 different genes have been identified to cause retinitis pigmentosa (see RetNet: https://sph.uth.tmc.edu/retnet/). Among these, Prominin-1 (PROM1, AC133, CD133, PROML1) is a promising candidate for the development a gene therapy. Particularly, children which are born with mutations in prominin-1 are of main interest for such therapy since their retina still contains a high amount of photoreceptors suitable for prominin-1 gene delivery. Prominin-1 is a 5-transmembrane-domain glycoprotein (Fig. 17A) located at plasma membrane protrusions and expressed in various tissues. Recent results indicate that Prominin-1, which is located at the tip of the connecting cilium, apical to the photoreceptor inner segment (IS), plays a central role in photoreceptor outer segment (OS) disc morphogenesis ([61], see also Fig. 17B).

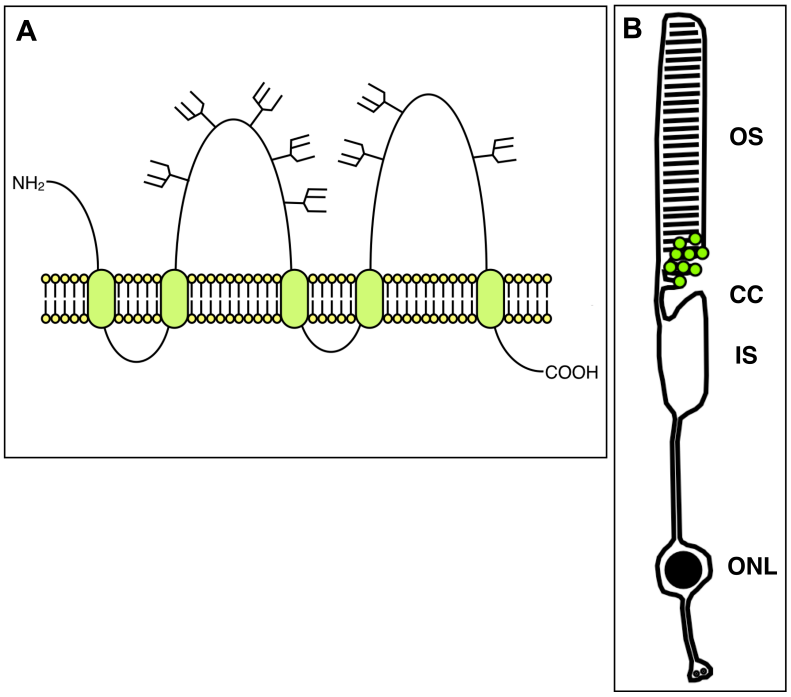

Figure 17: Prominin-1 - structure and cellular localization. Prominin-1, a 5-transmembrane domain glycoprotein (A) is expressed at the base of the outer segment (OS) of mature photoreceptor cells (B, cartoon of a rod cell). In this region, outer segment (OS) discs start to grow out and new disc membrane staples are formed.

To date, six different mutations in human prominin-1 are known, causing a variety of retinal degenerative disorders ranging from Stargardt-like via bull‘s eye macular dystrophy and cone-rod dystrophy to retinitis pigmentosa (Tab. 2). Five of the six mutations are known to be autosomal recessive with four of them affecting the open reading frame [62-65] and one, predicted to cause a splice defect [66]. The last one of the six mutations is reported to be autosomal dominant [67-70]. In focus of this study are the autosomal recessive mutations where the phenotype is caused by the absence or non-functional presence of the protein at its native final location, the plasma membrane.

For ocular gene delivery, recombinant adeno-associated viral (rAAV) vectors are most widely used and studied [8-10]. Their proven long-term transgene expression and the fact, that they may generate only minor immune responses, highlights them as ideal delivery vehicles. Different retinal cell types could be selectively addressed by using specific serotypes [71-73] and recent approaches focus on engineering new, artificial serotypes for even more specific targeting [74]. Functional rescue of photoreceptor cells in animal models of recessive Leber congenital amaurosis [75-77] and achromatopsia [78] as well as autosomal dominant [79,80], recessive [81] and X-linked retinitis pigmentosa [82] has been demonstrated recently.

Here, I follow these studies on the background of autosomal recessive Prominin-1 deficiencies. A delivery of wt prominin-1 to diseased host photoreceptor cells using rAAV vectors should theoretically lead to a rescue of the retinal degenerative phenotype. The animal model used in this study, the prominin-1 knock-out mouse, displays only disorganized OS discs and retinal degeneration [61]. Taken into account that prominin-1 is expressed in various cell types, including stem cells, this defined phenotype is a remarkable and unexpected finding and highlights the fact, that mutations and deletions of prominin-1 are only affecting photoreceptor cells. Retinal degeneration starts in prominin-1 knock-out mice at post-natal day 15 with an initially severe loss of ~50% of all

photoreceptor cells within 5 days while slowing down later in a logarithmic curve until total degeneration of the ONL with the age of 12 months [61]. This loss of photoreceptors over time mimics the phenotype known from human prominin-1 mutations. For the development of a gene therapy, I tested, whether it is possible to rescue the knock-out phenotype by delivering wt prominin-1 to the host photoreceptors using serotype 2/5 and 2/8 rAAV vectors.

autosomal dominant				
reported genomic locus	author	year	reported phenotype	PubMed ID
1117C>T	Yang Z	2008	macular degeneration	18654668
	Michaelides M	2010	bull's eye maculopathy associated with rod, rod-cone, and macular dystrophy	20393116
Chromosome 4p, 12-cM interval between loci D4S1582 and D4S2397, defined as STGD 4 locus	Kniazeva M	1999	stargardt-like disease	10205271
Chromosome 4p15.2-16.3, between loci D4S3023 and D4S3022, overlapping the STGD 4 locus	Michaelides M	2003	bull's-eye macular dystrophy	12657606
autosomal recessive				
reported genomic locus	author	year	reported phenotype	PubMed ID
1878delG	Maw MA	2000	retinal degereration	10587575
1726C>T	Zhang Q	2007	severe form of retinitis pigmentosa accompanied by macular degeneration	17605048
1349insT	Pras E	2009	cone-rod dystrophy and high myopia	19718270
869delG	Permanyer J	2010	retinitis pigmentosa with premature macular atrophy and myopia	20042663
1142-1G>A	Littink KW	2010	cone-rod dystrophy	20554613

Table 2: Reported human mutations in Prominin-1. Reported genomic loci from Kniazeva et al., 1999 and Michaelides et al., 2003 overlap at the STGD 4 locus and are most likely the same. This locus seems to be the 1117C>T locus reported by Yang et al., 2008 and Michaelides et al., 2010, later (Denis Corbeil, personal communication). This reduces the number of reported autosomal dominant human Prominin-1 mutations to one, whereas all five autosomal recessive mutations refer evidentially to different loci as reported by Maw et al., 2000; Zhang et al., 2007; Pras et al., 2009; Permanyer et al., 2010 and Littink et al., 2010. The 1142-1G>A mutation is predicted to impair splicing and is not affecting the open reading frame, like the other reported mutations.

4.2) Results

4.2.1) Targeting specificity and expression profile of rAAV-constructs

For viral vector therapies, vector targeting specificity and efficiency is of prime importance. Since AAV serotypes 2/5 and 2/8 have been shown to target photoreceptor cells [71-73], I tested them as GFP-expressing vectors, driven by an ubiquitously active CMV promoter with sub-retinal delivery on wild-type retinas. There, they display high photoreceptor specificity and a strong, injection-site restricted transgene expression with minor, non significant differences between them (Fig. 18B). In few cases (< 0.1%), single Müller-glia cells or second order neurons were targeted (see appendix Fig. S1). Under native conditions prominin-1 is selectively expressed at plasma membrane protrusions of various cell types, and in photoreceptors it is concentrated at the base of the OS (Fig. 18A) [63]. By transducing wt retinas with rAAV2/5 vectors expressing a prominin-1::GFP fusion construct, where GFP is translationally fused to the C-terminal domain of prominin-1, I could show an exclusive localization to the inner and the base of the OS in wild-type animals (Fig. 17C), which corresponds partly with the wt expression (compare Fig. 17A and C). In a previous study, it was demonstrated that GFP protein fused to the C-terminus of prominin-1 did not interfere with its proper targeting to plasma membrane protrusions such as microvilli of polarized epithelial cells [83]. The detection of prominin-1::GFP in ISs revealed its correct intracellular transport within cellular compartments (e.g. ER, Golgi) en route to the cell surface [83].

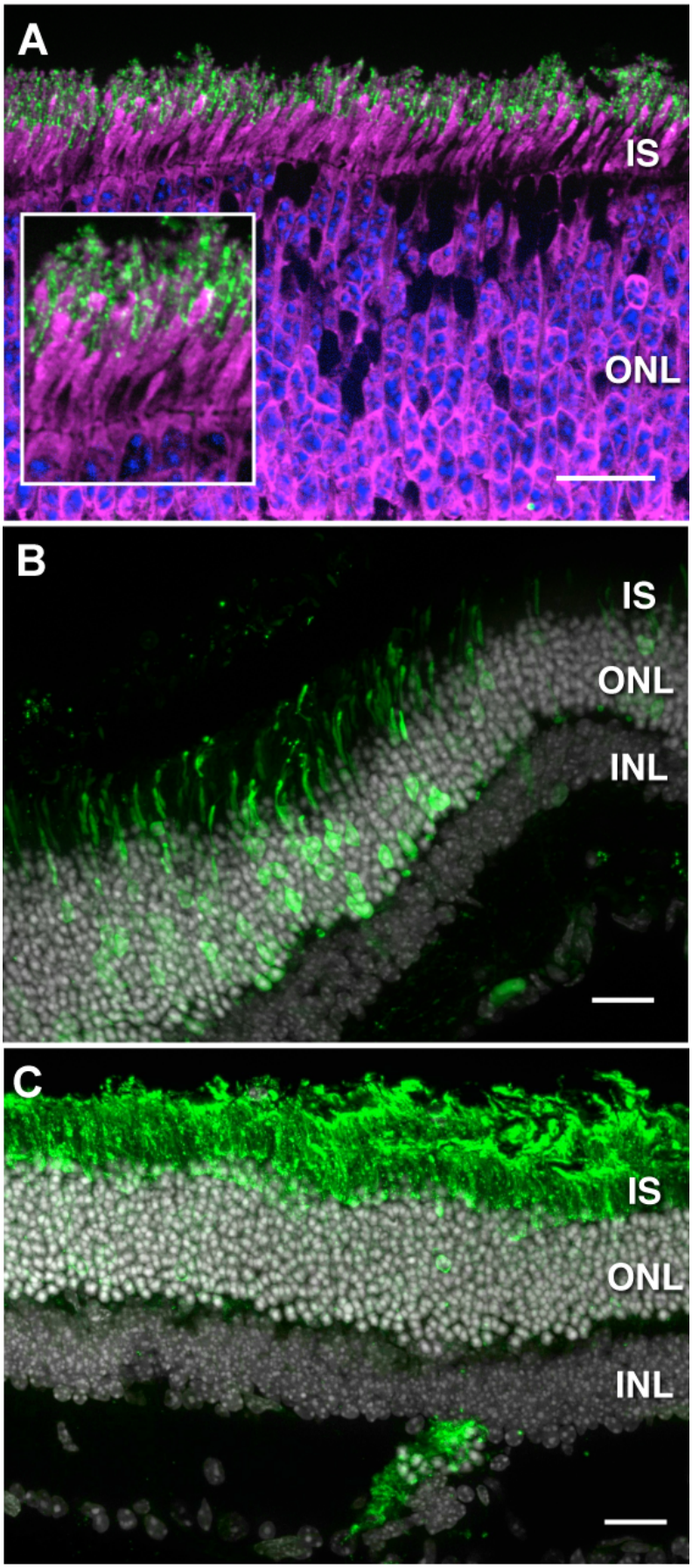

Figure 18: Prominin-1 expression and viral vector based delivery to a wild-type retina. Prominin-1 is expressed at the tip of the inner segment (IS) of mature photoreceptor cells, which can be labeled by recoverin (A, IS, magenta) The insert in A shows a high power image of the IS region. In this region, adjacent OS discs start to grow out and new disc membrane staples are formed. The transduction rate of rAAV2/5 and rAAV2/8 was tested with GFP-expressing vectors on wt retinas (B, green). In general, a transduction efficiency of approx. 50 - 80% of all host outer nuclear layer (ONL) cells could be achieved. With a specificity of 95 - 100% for photoreceptor cells, rAAV2/5 and rAAV2/8 vectors have proven them suitable for photoreceptor gene therapy. Proper translocation of the Prominin-1 construct to the outer segment was tested with a rAAV2/5-vector expressing a Prominin-1::GFP fusion protein. After sub-retinal delivery, strong GFP expression could be detected in ISs as well as in OSs (C, green) of host photoreceptor cells. INL: inner nuclear layer, A-C: 30 μm vibratome sections, scale bar: 20 μm

4.2.2) Short-term effects of prominin-1-delivery to the prominin-1 knock-out retina

The data obtained so far promoted me to investigate the possibility to rescue the retinal phenotype observed in prominin-1 knock-out mice. Remarkably, delivery of prominin-1 alone (i.e. without GFP fused to it) to a post-natal day 15 old prominin-1 knock-out mouse resulted in strong expression of Prominin-1 protein at its native sub-cellular location, i.e. the base of the photoreceptor OS, in contrast to results from prominin-1::GFP transductions (compare Fig. 18A and Fig. 19C“ with Fig. 18C). Prominin-1 expression was first detectable 2 weeks after injection (Fig. 19B). Morphological differences in ONL thickness between injected and non-injected eyes first occurred 3 weeks after injection (Fig. 19C). The results indicate a thicker ONL in the area of prominin-1 expression, compared to areas devoid of it within the same retina (Fig. 19C‘,C“). This leads to the conclusion that ectopic expression of prominin-1 in knock-out mice using rAAV-vector based delivery might rescue the effect of Prominin-1-deficiency resulting in photoreceptor survival and ONL preservation 3 weeks after treatment.

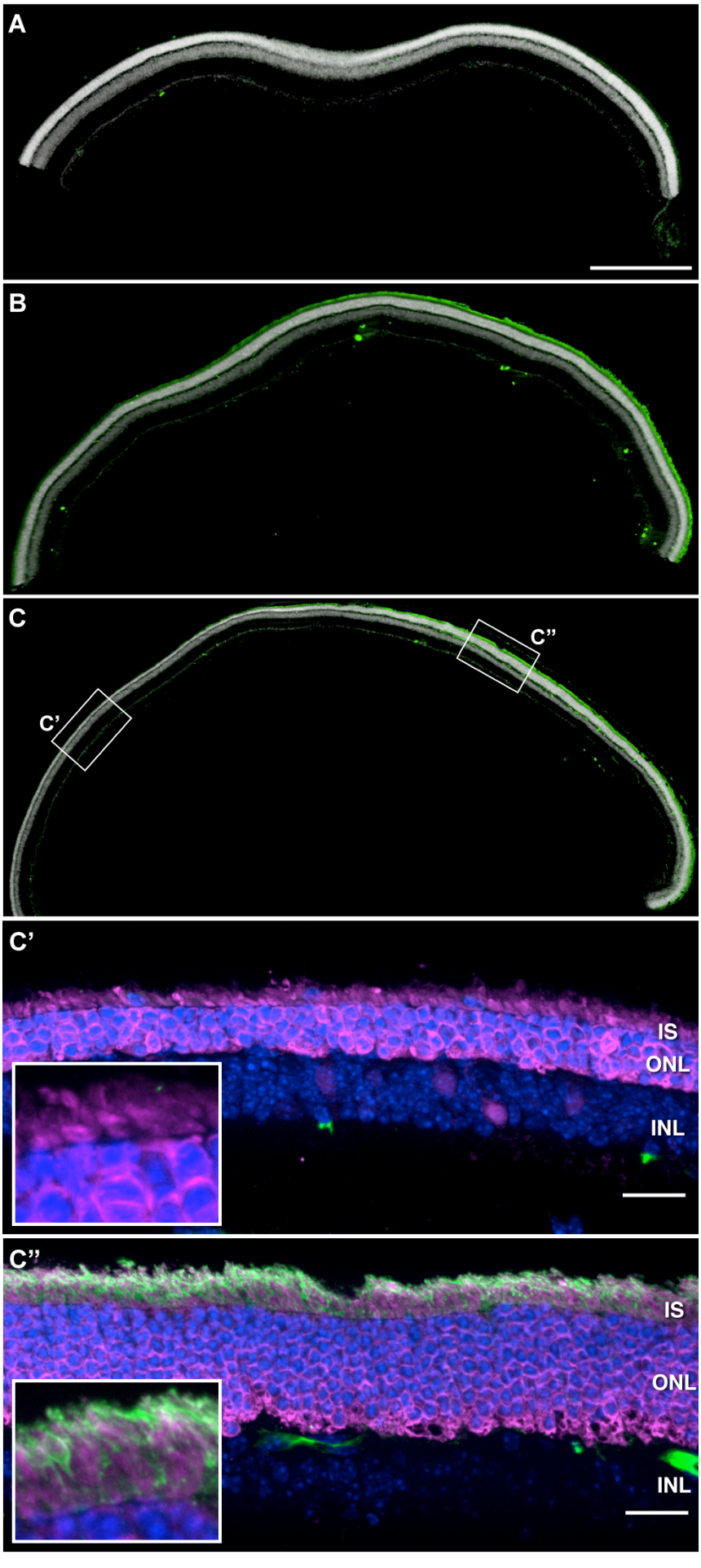

Figure 19: Prominin-1 delivery to the knock-out retina - 1-3 weeks post treatment. The expression of prominin-1 in knock-out mice was examined 1, 2 and 3 weeks after sub-retinal delivery to post-natal day 15 mice. It was evaluated whether its expression has any effect on ONL thickness, indicating photoreceptor survival or degeneration. After 1 week no expression was visible (A, green, nuclear marker DAPI in white) while after 2 weeks a strong anti-Prominin-1 antibody staining could be observed, covering approximately 1/3 of the retina (B, green). The ONL thickness decrease slightly from 1 to 2 weeks post injection (compare A and B, white). After 3 weeks, prominin-1 expression remains strong and restricted to the tip of the IS region (compare B and C, green). The thickness of the ONL remains unchanged in the area of prominin-1 expression (C”) compared with 2 weeks post injection, whereas in non-transduced areas of the same retina a strong decrease in ONL thickness could be observed (C’). This is consistent with the untreated, contralateral control eye (not shown), indicating a protective effect of prominin-1 expression. Inserts in C‘ and C‘‘ show magnifications of the inner segment region of respective pictures. IS: inner segment, ONL: outer nuclear layer, INL: inner nuclear layer; A-C“: 30 μm vibratome sections, scale bar: A-C: 200 μm, C’,C”: 20 μm

4.2.3) Long-term effects of prominin-1-delivery to the prominin-1 knock-out retina

ONL preservation by prominin-1 delivery to a knock-out retina was shown on a short time period (i.e. 3 weeks after injection). Nevertheless, for therapeutical purposes, it is absolutely necessary to show beneficial effects over a long period of time. To test this, we injected post-natal day 15 prominin-1 knock-out mice with rAAV2/8 vectors expressing native prominin-1. After 8 and 10 weeks, functionality of photoreceptors was tested by electroretinogram (ERG) before examination of the histological structure of the retinas (Fig. 20). Treated retinas displayed strong prominin-1 expression in the area of the ISs (Fig. 20A-H, green, IS stained by recoverin, magenta). In contrast to short-term results shown above, I could not detect beneficial effects in any of the treated eyes. Indeed, treated eyes displayed impaired photoreceptor morphology (highlighted by recoverin staining in Fig. 20A-H). This could be observed especially when comparing the IS structure between treated and untreated retinas (compare IS alignment and structure in Fig. 20A, C, E, G with B, D, F, H). Additionally, the thickness of the ONL was significantly thinner in treated eyes, compared to the contralateral untreated eye (compare ONL thickness in Fig. 20A, C, E, G with B, D, F, H). These results are in line with functional results obtained from ERG measurements. While untreated eyes displayed a reduced ERG signal (Fig. 20B‘, D‘ F‘, H‘) compared to a normal wt signal (Fig. 20K), treated eyes displayed an even more reduced signal (Fig. 20A‘, C‘ , E‘, G‘), compared to untreated eyes and the wt animal. Notably, within the population of treated eyes, stronger degenerated retinas (Fig. 20A, E) displayed almost no ERG signal (Fig. 20A‘, E‘) while weaker degenerated retinas (Fig. 20C, G) display at least a subtle signal in ERG measurements (Fig. 20C‘, G‘). This shows 1), that rAAV2/8 mediated prominin-1 therapy of prominin-1 knock-out mice resulted in negative effects on a long timescale, especially in respect to photoreceptor morphology and survival, and 2), that morphologically stronger degenerated retinas show weaker ERG signals, which indicates in this case, that functionality could be directly correlated with

ONL structure and photoreceptor integrity. Since not all injections are equal in success, there might be also a correlation in injection quality and long-term survival of photoreceptor cells. Indeed, eyes with injections which were rated in personal documentations as qualitatively good display better retinal structure and ERG signal (Fig. 20C, C‘ and G, G‘) than eyes with injections which were rated as qualitatively bad (Fig. 20A, A‘ and E, E‘). This highlights the importance of a save and minimal invasive ocular injection on the background of long-term retinal treatments in respect to viral vector deliveries as well as cell therapies.

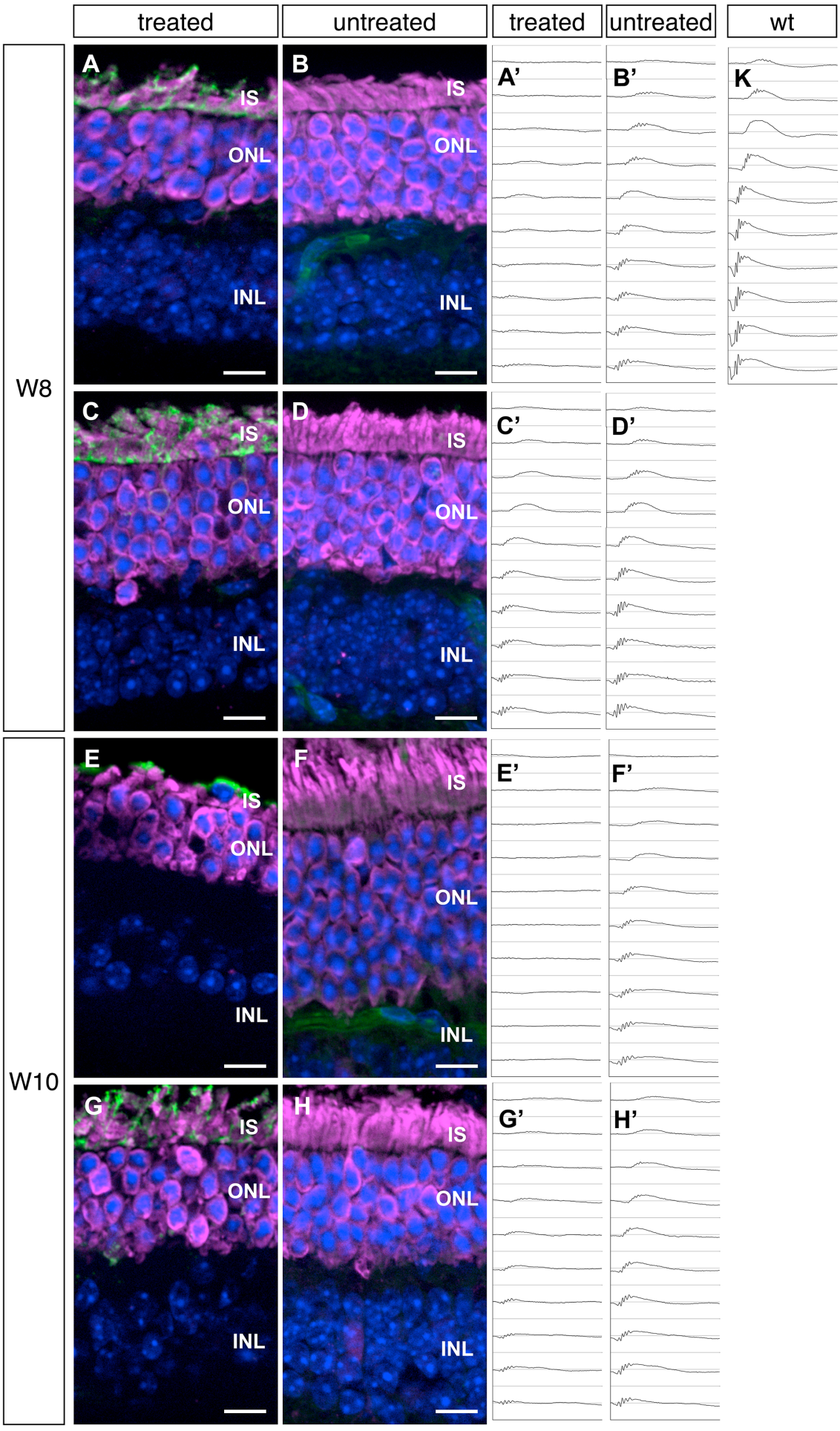

Figure 20: Long-term study for prominin-1 delivery to the knock-out retina - 8-10 weeks post treatment.

Figure 20: Long-term study for prominin-1 delivery to the knock-out retina - 8-10 weeks post treatment. Long-term effects of prominin-1-delivery to the prominin-1 knock-out host animal retina via rAAV2/8-mediated viral vector treatment were examined 8 (animal 1 A, B; animal 2 C, D) or 10 weeks (W) (animal 1 E, F; animal 2 G, H) after injection. Since every host mouse was transduced with the age of post-natal day 15, the mice were 10 or 12 weeks old, respectively, on the day of examination. Before examination, functional preservation of photoreceptor function was tested by electroretinogram (ERG, A‘-H‘, K: wt reference). In contrast to short-term results (see Fig. 18), long-term preservation could not be observed. Indeed, the delivery of prominin-1 (A-G, green) seem to have negative effects on photoreceptor morphology (A-D, recoverin staining in magenta) and survival (compare IS alignment and ONL thickness in A, C, E, G with B, D, F, H). This was verified by ERG measurements (compare A‘, C‘, E‘, G‘ with B‘, D‘, F‘, H‘). Note, that animals with strong degeneration profile on treated eyes (W8: A; W10: E) display almost no ERG signal (W8: A‘; W10: E‘) while animals with weaker degeneration (W8: C; W10: G) display a subtle ERG signal (W8: C‘; W10: G‘). Nevertheless, this signal was smaller than the non-treated contralateral eye (compare C‘ with D‘ and G‘ with H‘). IS: inner segment, ONL: outer nuclear layer, INL: inner nuclear layer, nuclear DAPI staining shown in blue, ERG signals are shown as μV / ms graphs under different stimulus intensities from top to bottom: 0.0003, 0.001, 0.003, 0.01, 0.03, 0.1, 0.3, 1, 3, 10 cd $\times$ s / m^2, scale bars: 10 μm.

4.3) Discussion

Inherited retinal degenerative diseases like retinitis pigmentosa account for a significant amount of blind people in the world. It has been shown, that mutations in prominin-1, a 5-transmembrane-domain glycoprotein expressed at plasma membrane protrusions, lead to severe visual impairment ranging from Stargardt-like via bull‘s eye macular dystrophy and cone-rod dystrophy to retinitis pigmentosa (Tab. 2). Viral vector based gene therapies represent today a promising tool for the treatment of inherited retinal diseases [8-10]. This study focusses on four of seven known mutations of prominin-1, which are known to be autosomal recessive [62-65]. There, the phenotype is caused by the absence or non-functional presence of the protein, which makes them suitable for a gene therapy based on the delivery of wt prominin-1 to the patients‘ photoreceptors.

To test the feasibility of such therapy, we delivered wt prominin-1 via rAAV-vectors to prominin-1 knock-out mouse retinas, which display retinal degeneration and disorganized disc membrane staples [61]. My initial studies showed, that the rAAV serotypes 2/5 and 2/8 display high photoreceptor specificity and strong transgene expression after sub-retinal delivery in wt animals. Additionally, the observed translocation of transduced prominin-1::GFP fusion constructs to the IS of wt photoreceptors indicates a native-like targeting of our construct. In short-term experiments, I could show that prominin-1, virally delivered to the prominin-1 knock-out retina, is specifically expressed in the host photoreceptors and expression could be observed at its native location, i.e. the base of the OS. First expression could be observed 2 weeks after injection and ONL thickness preservation could be detected 3 weeks after injection on a histological base.

In contrast to this, long-term studies revealed until now negative effects of this treatment. Experimental prominin-1 knock-out animals which were treated with rAAV2/8 viral vectors expressing wt prominin-1 were analyzed 8 or 10 weeks after using ERG measurements and histological sectioning. Histology revealed a thinner ONL and an

impaired photoreceptor IS integrity in treated versus untreated, contralateral retinas. This was verified by ERG measurements where treated eyes showed markedly reduced or no signal compared to untreated eyes. This indicates a negative effect of prominin-1 viral vector-based delivery on prominin-1 knock-out host photoreceptors on a long timescale, especially in respect to photoreceptor morphology and survival. This is in contrast to short-term results and indicates a negative effect, which establishes on a long timescale.

One reason might be the high-level transgene expression by the viral vector using a cytomegalie virus (CMV) promoter. In contrast to the native situation, where prominin-1-expression is driven by its own promoter regulating its expression level, in our therapeutical approach, prominin-1 might be over-expressed leading to an accumulation at the target location as well as neighboring membranes, like the IS, as observed in the long-term study as well as in prominin-1::GFP fusion construct experiments. This might be detrimental to IS structure as well as intra-cellular trafficking. Additionally, photoreceptors are remarkably specialized neuronal cells with high protein turnover and energy consumption. Therefore, the introduction of multiple copies of high level prominin-1-expressing CMV promoter constructs might affect photoreceptor cells already on low thresholds. Last but not least, there might be a day-night cycle in expression levels of native prominin-1 as reported from *Xenopus laevis* photoreceptors [84]. Since prominin-1 is closely connected to the formation of new discs, and these are known to be shedded and therefore renewed in a light dependent cyclic manner this seems to be highly probable and should be subject of further studies. The usage of the prominin-1 promoter might therefore mimic its native expression better than the constantly expressing CMV promoter. Future studies will focus on using the native prominin-1 promoter including testing of Prominin-1 protein levels per retina. This might result in native Prominin-1 levels at the right time in transduced cells of a prominin-1 knock-out retina and a survival of these cells, together with functional recovery.

The fact, that I could detect a direct correlation between ERG signal quality and ONL thickness as well as photoreceptor IS integrity, proves ERG measurements as a reliable tool to detect functional changes in ocular gene-therapeutical studies. Additionally I was able to detect a direct connection between the quality of injection and the integrity and survival rate of host photoreceptor cells. This indicates the importance of minimal invasive ocular delivery strategies, especially according to the treatment of patients with retinal degenerative diseases, where diseased photoreceptor cells might be more sensitive to surgical procedures, compared to healthy patients‘ photoreceptors.

5) Summary

Current studies follow a variety of different strategies to overcome permanent and, to date, incurable vision loss caused by retinal degenerative diseases. They could be generally classified as chemical, biological and technical approaches whereas some of them combine features from different disciplines (Fig. 21).

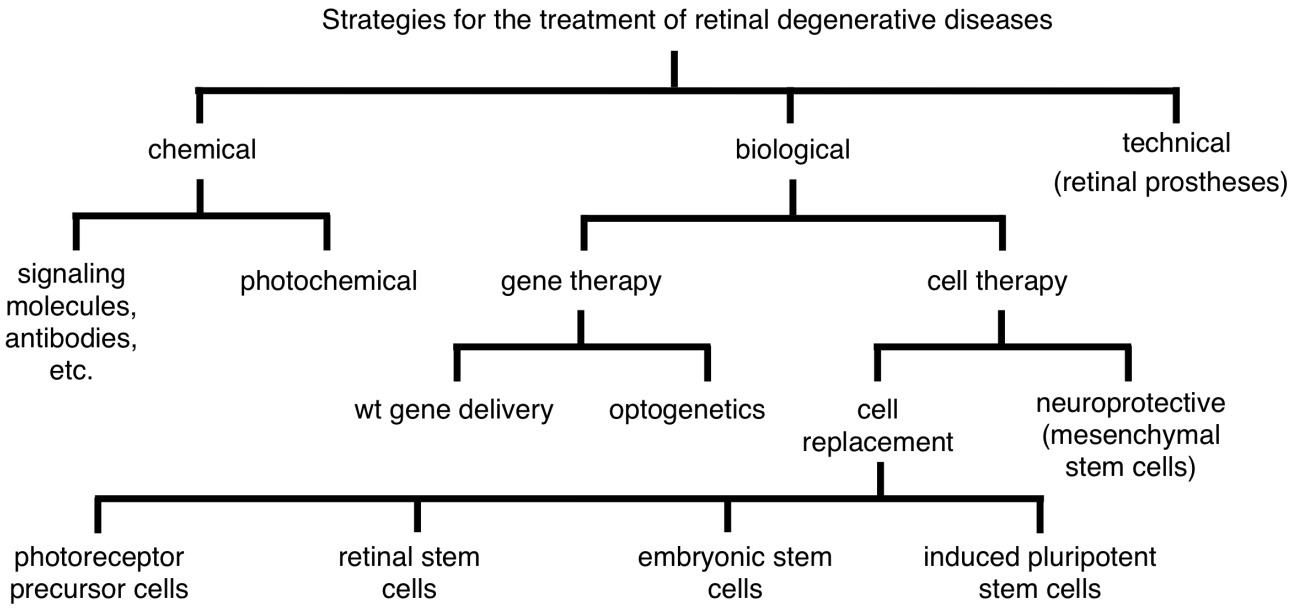

Figure 21: Overview of strategies for the treatment of retinal degenerative diseases.

Chemical approaches focus mainly on the usage of signaling molecules which have neuro-protective or growth-inducing effects and on antibodies for defined receptors to manipulate cell behavior. Neuro-protective and sub-cellular regenerative effects have been demonstrated for the treatment of retinal degeneration e.g. with the application of ciliary neurotrophic factor (CNTF) [85-87], human transferrin [88], curcumin [89], N-acetyl serotonin [90] and rare earth nanoparticles [91] mainly to the vitreus body of the eye. For the treatment of neovascular age-related macula degeneration (AMD), anti-vascular endothelial growth factor (VEGF) antibody therapy has been proven to treat successfully one major symptom (neovascularisation) resulting in a decrease in the rate of

degeneration [92,93]. A recent elegant approach combines chemistry with photosensitivity by applying a photochemical active small molecule “photoswitch“ to the retina of blind mice resulting in restored light responsiveness [94].

While most of the chemical approaches may be beneficial only in early disease stages retinal prosthesis approaches represent a technical solution applicable to a severely degenerated retina. The principle of this strategy is the replacement of degenerated photoreceptor cells by electronic chip implants which detect light and stimulate the remaining retinal cells via electric signals [95]. These studies are in advanced stages and some prostheses are already tested in clinical trials [34,96,97]. Recent advances in this field focus on the optimization of these prostheses in respect to resolution [98] or independence from external power sources [99].

Beside chemical and technical approaches, biological approaches represent a promising field where protecting, restoring or regenerative therapies might be established soon. They could be divided into cell therapies and gene therapies. One gene therapeutic field with intensive research focuses on optogenetic approaches [100] following the idea, that the remaining neuronal cells in a photoreceptor-depleted, degenerated retina can be turned into light-sensing cells by transgenic expression of opsins [101]. Recent work demonstrates the restoration of visual responses by introducing microbial channel-rhodopsins [102,103] or melanopsin [104] in retinal ganglion cells (RGCs) or channelrhodopsin in ON bipolar cells [105,106] as well as by introducing archaebacterial halorhodopsin in light-insensitive, remaining cones in a severely degenerated RP retina [107].

While optogenetic approaches focus on late-stage diseases, general gene therapeutical approaches have to be applied at early stages, when photoreceptors are still left. The principle of an ocular gene therapy focusses on hereditary retinal degenerations and the fact, that a mutated gene, which leads to retinal degeneration, can be replaced by

a vector-delivered wt gene which results in a cure of the disease at it‘s “root“. AAV-vectors have been proven to be the most effective and reliable tool for this task, to date [8-10]. Functional rescue has been demonstrated in animal models of autosomal dominant [79,80], recessive [81] and X-linked retinitis pigmentosa [82] as well as recessive Leber congenital amaurosis [75-77] and achromatopsia [78].

While first gene therapies for retinal inherited diseases are already in clinical trials [108], another strategy, the cell therapy approach, is still in its infancy. In one branch of a cell therapy, helper cells like mesenchymal stem cells (MSCs) are transplanted to the retina or the vitreus body [109]. Their neuroprotective properties are topic of current research e.g. in animal models of glaucoma where they elicit this effect by native paracrine neurotrophic factor secretion [110] or as genetically modified cells by brain-derived neurotrophic factor release [111].

Researchers following another branch of retinal cell therapy focus on replacing degenerated photoreceptor cells by sub-retinal injected wt photoreceptor source cells, which integrate in the remaining, or form a new photoreceptor layer. These photoreceptor source cells are the topic of current research and controversial discussions. For PPCs, isolated from post-natal day 4 retinas, successful transplantation and integration has been shown [15,16] but *in vitro* expansion without losing their PPC state has not been reported until now. Several groups investigated the potential of expandable cells isolated from the retina, the so-called “retinal stem cells” [56-59], pluripotent stem cells, i.e. ESCs [18,24] or iPS cells [25,42,60] with different success in outcome. Currently, ESCs elicit the highest potential to be a reliable, stable and successful source for PPCs, whereas, because of ethical concerns, iPS cells might be the best choice for the future.

Like optogenetic approaches, photochemical treatments and retinal prostheses, a photoreceptor cell replacement therapy implies the advantage, that diseases like RP, with common phenotype, but a variety of genes that might be mutated, may be cured at once,

here specifically by introducing new, genetically native PPCs. In these cases, a gene therapy has to be developed for each gene that is mutated and therefore for each group of patients that are affected. Also, gene therapy requires remaining viable host photoreceptor cells, whereas a photoreceptor cell replacement therapy might be applicable in severely degenerated retinas. Another advantage of this therapy in contrast to optogenetic approaches, photochemical treatments or retinal prostheses is, that an optimal, native resolution of the eye with almost one hundred million photoreceptors [2] may only be achieved in near future by introducing new photoreceptor cells to a diseased retina. In comparison, the current maximal resolution of optogenetic or photochemical therapies is limited by the number of remaining neurons, whereas a stimulation of RGCs with already processed optical signals represents a promising strategy to overcome this problem [98]. In line with optogenetics and photochemical treatment, retinal prostheses share the disadvantage of currently low resolution. Also here, research is made to improve the density of electrodes to increase the amount of pixels. Nevertheless, a stable and proven retinal cell therapy represents the most promising treatment for high quality vision gain in retinal degenerative diseases, to date.

Summing up, this study shows, that with pre-transplantational sorting, using the PPC-specific cell surface marker CD73, a significant enhancement of the integration rate of PPCs in wt host retinas can be achieved. Next to this quantitative approach, it is also shown that the quality of transplanted PPCs is comparable to native photoreceptors by demonstrating, that an indispensable prerequisite of every photoreceptor cell, the OS, is developed by transplanted PPCs after integration and even when not integrated and sub-retinal located. Additionally, I could show, that this is not the case when PPCs are transplanted to the vitreal side of the retina, suggesting an influence of signaling molecules presumably secreted by RPE cells into the sub-retinal space.

Last, but not least, the gene therapeutical part of this work demonstrates, that a treatment of prominin-1 mutations-derived retinal degenerative diseases with the use of recombinant AAV vectors by delivering native prominin-1 selectively to the patients‘ photoreceptor cells might be possible. The divergent results show on one hand a rescue of the thickness of the photoreceptor ONL on a short time period, and on the other hand long-term data suggests histologically as well as functionally a negative effect on treated eyes. This might be due to effects caused by an over-expression of prominin-1 and will be investigated in further studies.

In conclusion, distinct and important investigations were made which contribute significant puzzle pieces to new cell- as well as gene therapeutical approaches for the treatment of retinal degenerative disorders.

6) Material and Methods

Ethics Statement

All animal experiments were carried out in strict accordance with European Union and German laws (Tierschutzgesetz) and adhered to the ARVO Statement for the Use of Animals in Ophthalmic and Vision Research. All animal experiments were approved by the animal ethics committee of the TU Dresden and the Landesdirektion Dresden (approval number: 24D-9168.11-1/2008-33).

Animals

Donor cells were isolated from retinas of PN4 transgenic reporter mice. The first transgenic animal used is characterized by the expression of EGFP fused to human rhodopsin, which is introduced into the mouse rhodopsin locus (rhoEGFP mice) [33]. This reporter fusion protein facilitates the selective labeling and tracking of OS development since rhodopsin is specifically located therein. The second reporter mouse line was generated by crossing the rhoEGFP mouse line with the actin-DsRed one, in which DsRed expression is driven by an ubiquitous active chicken beta-actin promoter (DsRed, B6.Cg-Tg(CAG-DsRed*MST)1Nagy/J from The Jackson Laboratory, Maine, USA; [112]). This double reporter mouse line allows the tracking of transplanted PPCs simultaneously to the development of their OSs in host retinas. The third reporter mouse line is the Nrl-EGFP line [113]. In Nrl-EGFP mice a transgene coding for EGFP driven by the Nrl promoter was introduced. Nrl is a transcription factor determining the rod fate and the earliest known marker for rod photoreceptors. Donor cells were either transplanted into wild-type mice (C57BL/6J; age: 2 – 4 months) or heterozygous P347S mice (age: 4 and 12 weeks, n = 5), a model for autosomal-dominant RP [50]. For light-sensitivity studies, PN4, CD73-positive

sorted actinDsRed, rhoEGFP double reporter donor cells were transplanted into P347S mice (age: 10 weeks, n=4), which were light-adapted (10h in normal ambient light) or dark-adapted (24h in complete darkness) 4 weeks after transplantation.

Magnetic-activated cell sorting (MACS)

PPCs were enriched from 4-days old reporter mouse retinas using CD73 as a cell surface marker and immuno-paramagnetic separation methods as reported [30]. In brief, isolated retinas were dissociated, pelleted and dissolved in MACS buffer (Miltenyi Biotec, Bergisch Gladbach, Germany). After incubation with rat anti-CD73 antibodies (BD Pharmingen, Heidelberg, Germany), cells were washed and incubated with secondary anti-rat antibodies coupled with magnetic beads (Miltenyi Biotec), followed by a second washing step and filtering through a 30-μm pre-separation filter. Afterwards, magnetic separation was performed according to the manufacturer's protocol (Miltenyi Biotec). The CD73–positive cell fraction was collected and used for transplantations.

Recombinant adeno-associated virus vector (rAAV) preparation

The mouse prominin-1 gene (GenBank Acc. No. AF026269) was provided by Denis Corbeil (Biotec, TU Dresden) as insert in pRC/CMV vector (Invitrogen). Recombinant rAAV vectors were created by Prof. Regine Heilbronn and Dr. Stefan Weger (Charité, Berlin). Briefly, HEK-293 cells were infected with packaging constructs containing the transgene (prominin-1 or GFP or prominin-1::GFP) together with helper constructs containing the respective AAV Rep and Cap gene for serotypes 2/5 and 2/8 as well as adenoviral helper genes. The transgene transcripts are driven by an ubiquitously active cytomegalie virus (CMV) promotor (see also appendix Figs. S2-S4).

Immunohisto/cytochemistry

Whole mouse eyes were extracted from animals and processed as described in Eberle et al., 2011 [30]. Briefly, after fixation in 4% paraformaldehyde (PFA), the retina was dissected out and sectioned into 30-μm thick slices using a vibrating microtome (model 1200; Leica, Wetzlar, Germany). To visualize cell nuclei, samples were stained with 4',6-diamidino-2-phenylindole (DAPI; 1:10,000; Sigma-Aldrich, Munich, Germany). For immuno-staining fixed samples were blocked (30min) in PBS containing 5% goat serum (Sigma), 1% bovine serum albumin (BSA; Sigma), and 0.3% Triton X-100 (TU-Dresden pharmacy, Dresden, Germany), and incubated (4°C o/n) with the following primary antibodies: mouse anti-rhodopsin (rho4D2; 1:100; kind gift of R. Molday, University of British Columbia, Vancouver, BC, Canada or anti-Ret-P1, Sigma-Aldrich, Munich, Germany), rabbit anti-recoverin (1:3000; Millipore, Schwalbach, Germany) or rabbit anti-transducin (anti-$G_{\alpha\ t1}$, Santa Cruz Biotechnology, Santa Cruz, USA) antibodies. Primary antibodies were visualized by incubation (2h) with Cy2, Cy3 or Cy5-conjugated goat anti-mouse, anti-rabbit, or anti-rat secondary antibodies (Jackson Immunoresearch, West Grove, USA), respectively. Retinal sections were mounted on glass slides with AquaPolymount (Polysciences, Inc., Warrington, PA, US) for image acquisition.

Transplantation / Transduction

For transplantation of cell suspensions into the sub-retinal or vitreal space, adult (i.e. 2 – 4 months old) wild-type (C57BL/6J) or heterozygous P347S (4 – 12 weeks old) mice, and for injection of viral vector suspension in post-natal day 15 wild-type (C57BL/6J) or Prominin-1 knock-out animals (AC133-/-), mice were anesthetized by an intra-peritoneal injection of medetomidine hydrochloride (Dormitor®, Pfizer, Berlin, Germany; 0.01mg/10g body weight) and ketamine (Ratiopharm, Ulm, Germany; 0.75mg/10g body weight) and fixed in a head holder. Pupils were dilated by applying a drop of 1% tropicamid (Mydrum®, Dr.

Mann Pharma GmbH, Berlin, Germany) and 2.5% phenylephrine (TU-Dresden pharmacy). A Hamilton syringe with a blunt 34-gauge needle was inserted tangentially through the conjunctiva and sclera and placed under visual control into the sub-retinal space, i.e. between the retina and RPE producing a bullous retinal detachment, or into the vitreal space, i.e. in front of the ganglion cell layer. 1 μl of cell suspension containing approximately 400,000 cells or 1μl of viral vector suspension containing approximately 2-8 x 10^{11} GP/ml was injected per eye. The viral vectors were always applied sub-retinal while cell suspensions were applied sub-retinal and / or vitreal, dependent on the type of experiment. For recovery, experimental animals received an injection of atipamozole hydrochloride (Antisedan®, Pfizer, 0.1mg/10g body weight) for reversal of medetomidine.

Quantification of integrated photoreceptors

Three weeks after transplantation experimental animals were sacrificed and the eyes were removed and fixed in 4% PFA in PBS for 12h. Retinae were dissected out and embedded in 4% agarose to produce 30μm thick serial sections using a vibrating microtome (Leica 1200, Leica, Germany). Beside morphological criteria like a cell body located in the ONL and the generation of spherule synapses and/or inner segments integrated donor photoreceptors were identified by their red (DsRed in the cell body) and green (EGFP in the outer segments) fluorescence. For quantification seven retinae that received unsorted cell fractions, six retinae that received CD73-negative fractions, and seven retinae that received CD73-positive fractions were analyzed. The number of integrated donor cells per retina was calculated following quantification of every fourth serial section with a total of 18 sections per experimental retina using a Z1-Imager fluorescence microscope with ApoTome (Zeiss).

Electro-retinogram (ERG) measurements

ERG measurements were done with the Roland Consult Ganzfeld ERG Q450 system (Roland Consult, Brandenburg an der Havel, Germany) with animal table A1 adapter for mouse ERG investigations. After dark adaption for at least 12h, animals were kept for the whole ERG procedure in a dark room with red light. They were anesthetized as described above (see Transplantation / Transduction), placed at the table and connected to the respective electrodes. After checking the correct impedance, a scotopic Ganzfeld ERG series was launched with stimulus intensities ranging from 0.0003 - 10 cd $\times$ s / m^2. Finally, animals received an injection of atipamozole hydrochloride as described above (see Transplantation / Transduction) for reversal of anesthesia.

Correlative light and electron microscopy (CLEM)

Retina pieces were fixed with 4% PFA in 0.1 M phosphate buffer (PB, pH 7.4) overnight at 4°C. Fixed samples were processed for PLT-embedding in K4M as described [45,46]. In brief, samples were dehydrated in a graded series of ethanol at progressively lower temperatures, infiltrated in mixtures of ethanol/K4M at -35°C and embedded in resin. Polymerization occurred via UV-irradiation at -35°C. Ultra-thin sections were used for immunofluorescence and/or immuno-EM [45-47,114]. Sections were blocked with 1% BSA in PBS, incubated with rabbit anti-GFP (TP 401 from Torrey Pines or ab 290 from Abcam) followed by either Alexa488 (or Alexa555) conjugated secondary antibodies or by protein A 10-nm gold, and finally counterstained with DAPI (1 μg / ml). For CLEM of the very same section, ultra-thin sections were mounted on nickel finder grids (200 mesh, EMS, # G 200F1-Ni) and stained with anti-GFP antibody and protein A gold. After post-fixation with 1% glutaraldehyde / PBS, the sections were incubated with goat anti-rabbit Alexa488 and counterstained with DAPI. Labeled EM-grids were mounted between two coverslips in 50% glycerin/water [114] and analyzed at the fluorescence microscope, then de-mounted,

washed several times in water and stained with aqueous uranyl acetate before EM inspection.

Image acquisition and data analysis

Light microscopical images were taken using a Z1-Imager fluorescence microscope with Apotome and AxioCam Mrm camera (Zeiss, Germany). Before EM image acquisition, the fluorescence of CLEM samples was imaged using a Keyence BZ 8000 (Keyence, Neu-Isenburg, Germany). EM sections were analyzed using a Philips Morgagni 268 (FEI; Philips, Amsterdam, Netherlands) at 80kV and images were taken with the MegaView III digital camera (Olympus, Hamburg, Germany). Images were analyzed and prepared for publication using ImageJ, AxioVision (Zeiss), GNU Image Manipulation Program (Gimp) and iWork Keynote (Apple). Statistical data were analyzed using Microsoft Office Excel (Microsoft), or iWork Numbers (Apple) software. Results are presented as ± SEM (standard error of the mean) from at least three independent experiments. Significance was calculated by unpaired, 2-tailed, student's T-test and presented in figures by *$p<0.05$, **$p<0.01$, ***$p<0.001$.

7) Bibliography

1. Darwin C On the Origin of Species by Means of Natural Selection, Or, The Preservation of Favored Races in the Struggle for Life: Project Gutenberg. 242p. p.
2. Curcio CA, Sloan KR, Kalina RE, Hendrickson AE (1990) Human photoreceptor topography. J Comp Neurol 292: 497-523.
3. Brown PK, Wald G (1963) Visual Pigments in Human and Monkey Retinas. Nature 200: 37-43.
4. Carter-Dawson LD, LaVail MM (1979) Rods and cones in the mouse retina. I. Structural analysis using light and electron microscopy. J Comp Neurol 188: 245-262.
5. Berson DM (2007) Phototransduction in ganglion-cell photoreceptors. Pflugers Arch 454: 849-855.
6. Zhang DQ, Wong KY, Sollars PJ, Berson DM, Pickard GE, et al. (2008) Intraretinal signaling by ganglion cell photoreceptors to dopaminergic amacrine neurons. Proc Natl Acad Sci U S A 105: 14181-14186.
7. Hamel C (2006) Retinitis pigmentosa. Orphanet journal of rare diseases 1: 40.
8. Buch PK, Bainbridge JW, Ali RR (2008) AAV-mediated gene therapy for retinal disorders: from mouse to man. Gene Ther 15: 849-857.
9. Alexander JJ, Hauswirth WW (2008) Adeno-associated viral vectors and the retina. Adv Exp Med Biol 613: 121-128.
10. Surace EM, Auricchio A (2008) Versatility of AAV vectors for retinal gene transfer. Vision Res 48: 353-359.
11. Gouras P, Du J, Kjeldbye H, Kwun R, Lopez R, et al. (1991) Transplanted photoreceptors identified in dystrophic mouse retina by a transgenic reporter gene. Invest Ophthalmol Vis Sci 32: 3167-3174.
12. Gouras P, Du J, Kjeldbye H, Yamamoto S, Zack DJ (1992) Reconstruction of degenerate rd mouse retina by transplantation of transgenic photoreceptors. Invest Ophthalmol Vis Sci 33: 2579-2586.
13. Gouras P, Du J, Kjeldbye H, Yamamoto S, Zack DJ (1994) Long-term photoreceptor transplants in dystrophic and normal mouse retina. Invest Ophthalmol Vis Sci 35: 3145-3153.
14. Kwan AS, Wang S, Lund RD (1999) Photoreceptor layer reconstruction in a rodent model of retinal degeneration. Experimental neurology 159: 21-33.

15. MacLaren RE, Pearson RA, MacNeil A, Douglas RH, Salt TE, et al. (2006) Retinal repair by transplantation of photoreceptor precursors. Nature 444: 203-207.
16. Bartsch U, Oriyakhel W, Kenna PF, Linke S, Richard G, et al. (2008) Retinal cells integrate into the outer nuclear layer and differentiate into mature photoreceptors after subretinal transplantation into adult mice. Exp Eye Res 86: 691-700.
17. Lakowski J, Baron M, Bainbridge J, Barber AC, Pearson RA, et al. (2010) Cone and rod photoreceptor transplantation in models of the childhood retinopathy Leber congenital amaurosis using flow-sorted Crx-positive donor cells. Hum Mol Genet 19: 4545-4559.
18. Lamba DA, Gust J, Reh TA (2009) Transplantation of human embryonic stem cell-derived photoreceptors restores some visual function in Crx-deficient mice. Cell Stem Cell 4: 73-79.
19. Pearson RA, Barber AC, Rizzi M, Hippert C, Xue T, et al. (2012) Restoration of vision after transplantation of photoreceptors. Nature.
20. West EL, Pearson RA, Tschernutter M, Sowden JC, MacLaren RE, et al. (2008) Pharmacological disruption of the outer limiting membrane leads to increased retinal integration of transplanted photoreceptor precursors. Exp Eye Res 86: 601-611.
21. Pearson RA, Barber AC, West EL, MacLaren RE, Duran Y, et al. (2010) Targeted disruption of outer limiting membrane junctional proteins (Crb1 and ZO-1) increases integration of transplanted photoreceptor precursors into the adult wild-type and degenerating retina. Cell Transplant 19: 487-503.
22. West EL, Pearson RA, Barker SE, Luhmann UF, Maclaren RE, et al. (2010) Long-term survival of photoreceptors transplanted into the adult murine neural retina requires immune modulation. Stem Cells 28: 1997-2007.
23. Yao J, Feathers KL, Khanna H, Thompson D, Tsilfidis C, et al. (2011) XIAP therapy increases survival of transplanted rod precursors in a degenerating host retina. Investigative ophthalmology & visual science 52: 1567-1572.
24. Lamba DA, Karl MO, Ware CB, Reh TA (2006) Efficient generation of retinal progenitor cells from human embryonic stem cells. Proceedings of the National Academy of Sciences of the United States of America 103: 12769-12774.
25. Lamba DA, McUsic A, Hirata RK, Wang PR, Russell D, et al. (2010) Generation, purification and transplantation of photoreceptors derived from human induced pluripotent stem cells. PLoS One 5: e8763.

26. Osakada F, Ikeda H, Mandai M, Wataya T, Watanabe K, et al. (2008) Toward the generation of rod and cone photoreceptors from mouse, monkey and human embryonic stem cells. Nature biotechnology 26: 215-224.
27. Meyer JS, Shearer RL, Capowski EE, Wright LS, Wallace KA, et al. (2009) Modeling early retinal development with human embryonic and induced pluripotent stem cells. Proceedings of the National Academy of Sciences of the United States of America 106: 16698-16703.
28. Koso H, Minami C, Tabata Y, Inoue M, Sasaki E, et al. (2009) CD73, a novel cell surface antigen that characterizes retinal photoreceptor precursor cells. Investigative ophthalmology & visual science 50: 5411-5418.
29. Lakowski J, Han YT, Pearson RA, Gonzalez-Cordero A, West EL, et al. (2011) Effective transplantation of photoreceptor precursor cells selected via cell surface antigen expression. Stem Cells 29: 1391-1404.
30. Eberle D, Schubert S, Postel K, Corbeil D, Ader M (2011) Increased integration of transplanted CD73-positive photoreceptor precursors into adult mouse retina. Investigative ophthalmology & visual science 52: 6462-6471.
31. Edgar R, Domrachev M, Lash AE (2002) Gene Expression Omnibus: NCBI gene expression and hybridization array data repository. Nucleic acids research 30: 207-210.
32. Akimoto M, Cheng H, Zhu D, Brzezinski JA, Khanna R, et al. (2006) Targeting of GFP to newborn rods by Nrl promoter and temporal expression profiling of flow-sorted photoreceptors. Proc Natl Acad Sci U S A 103: 3890-3895.
33. Chan F, Bradley A, Wensel TG, Wilson JH (2004) Knock-in human rhodopsin-GFP fusions as mouse models for human disease and targets for gene therapy. Proc Natl Acad Sci U S A 101: 9109-9114.
34. Zrenner E, Bartz-Schmidt KU, Benav H, Besch D, Bruckmann A, et al. (2011) Subretinal electronic chips allow blind patients to read letters and combine them to words. Proceedings Biological sciences / The Royal Society 278: 1489-1497.
35. Thomson LF, Ruedi JM, Glass A, Moldenhauer G, Moller P, et al. (1990) Production and characterization of monoclonal antibodies to the glycosyl phosphatidylinositol-anchored lymphocyte differentiation antigen ecto-5'-nucleotidase (CD73). Tissue antigens 35: 9-19.
36. Colgan SP, Eltzschig HK, Eckle T, Thompson LF (2006) Physiological roles for ecto-5'-nucleotidase (CD73). Purinergic signalling 2: 351-360.

37. Singhal S, Lawrence JM, Bhatia B, Ellis JS, Kwan AS, et al. (2008) Chondroitin sulfate proteoglycans and microglia prevent migration and integration of grafted Muller stem cells into degenerating retina. Stem Cells 26: 1074-1082.
38. Suzuki T, Mandai M, Akimoto M, Yoshimura N, Takahashi M (2006) The simultaneous treatment of MMP-2 stimulants in retinal transplantation enhances grafted cell migration into the host retina. Stem Cells 24: 2406-2411.
39. Suzuki T, Akimoto M, Imai H, Ueda Y, Mandai M, et al. (2007) Chondroitinase ABC treatment enhances synaptogenesis between transplant and host neurons in model of retinal degeneration. Cell transplantation 16: 493-503.
40. Gust J, Reh TA (2011) Adult donor rod photoreceptors integrate into the mature mouse retina. Investigative ophthalmology & visual science 52: 5266-5272.
41. Redenti S, Neeley WL, Rompani S, Saigal S, Yang J, et al. (2009) Engineering retinal progenitor cell and scrollable poly(glycerol-sebacate) composites for expansion and subretinal transplantation. Biomaterials 30: 3405-3414.
42. Tucker BA, Park IH, Qi SD, Klassen HJ, Jiang C, et al. (2011) Transplantation of adult mouse iPS cell-derived photoreceptor precursors restores retinal structure and function in degenerative mice. PLoS One 6: e18992.
43. Gouras P, Du J, Gelanze M, Kwun R, Kjeldbye H, et al. (1991) Transplantation of photoreceptors labeled with tritiated thymidine into RCS rats. Invest Ophthalmol Vis Sci 32: 1704-1707.
44. Gouras P, Du J, Gelanze M, Lopez R, Kwun R, et al. (1991) Survival and synapse formation of transplanted rat rods. J Neural Transplant Plast 2: 91-100.
45. Schwarz H, and Humbel, B. M. (2009) Correlative light and electron microscopy. In: A. Cavalier DS, B. M. Humbel, eds., editor. Hand Book of Cryo-Preparation Methods for Electron Microscopy: CRC Press, Boca Raton. pp. pp. 537-565.
46. Schwarz H, Humbel BM (2007) Correlative light and electron microscopy using immunolabeled resin sections. Methods Mol Biol 369: 229-256.
47. Fabig G, Kretschmar S, Weiche S, Eberle D, Ader M, et al. (2012) Labeling of ultrathin resin sections for correlative light and electron microscopy. Methods in cell biology 111: 75-93.
48. Barber AC, Hippert C, Sowden JC, Ali RR, Pearson RA (2011) Retinal Repair In The Degenerating Retina: Assessing Photoreceptor Transplantation In Models Of Retinal Disease. ARVO Meeting Abstracts 52: 4019.

49. Hippert C, Barber AC, Georgiadis A, Bainbridge JW, Smith AJ, et al. (2012) Modulation Of Gliosis Using shGFAP Or/and shvimentin To Determine Its Role In Photoreceptor Transplantation Efficiency. ARVO Meeting Abstracts 53: 2010.
50. Li T, Snyder WK, Olsson JE, Dryja TP (1996) Transgenic mice carrying the dominant rhodopsin mutation P347S: evidence for defective vectorial transport of rhodopsin to the outer segments. Proc Natl Acad Sci U S A 93: 14176-14181.
51. Gaur VP, Liu Y, Turner JE (1992) RPE conditioned medium stimulates photoreceptor cell survival, neurite outgrowth and differentiation in vitro. Experimental eye research 54: 645-659.
52. Raymond SM, Jackson IJ (1995) The retinal pigmented epithelium is required for development and maintenance of the mouse neural retina. Current biology 5: 1286-1295.
53. Sheedlo HJ, Nelson TH, Lin N, Rogers TA, Roque RS, et al. (1998) RPE secreted proteins and antibody influence photoreceptor cell survival and maturation. Brain research Developmental brain research 107: 57-69.
54. Stiemke MM, Landers RA, al-Ubaidi MR, Rayborn ME, Hollyfield JG (1994) Photoreceptor outer segment development in Xenopus laevis: influence of the pigment epithelium. Developmental biology 162: 169-180.
55. Lin N, Fan W, Sheedlo HJ, Aschenbrenner JE, Turner JE (1996) Photoreceptor repair in response to RPE transplants in RCS rats: outer segment regeneration. Current eye research 15: 1069-1077.
56. Tropepe V, Coles BL, Chiasson BJ, Horsford DJ, Elia AJ, et al. (2000) Retinal stem cells in the adult mammalian eye. Science 287: 2032-2036.
57. Klassen HJ, Ng TF, Kurimoto Y, Kirov I, Shatos M, et al. (2004) Multipotent retinal progenitors express developmental markers, differentiate into retinal neurons, and preserve light-mediated behavior. Investigative ophthalmology & visual science 45: 4167-4173.
58. Coles BL, Angenieux B, Inoue T, Del Rio-Tsonis K, Spence JR, et al. (2004) Facile isolation and the characterization of human retinal stem cells. Proceedings of the National Academy of Sciences of the United States of America 101: 15772-15777.
59. Merhi-Soussi F, Angenieux B, Canola K, Kostic C, Tekaya M, et al. (2006) High yield of cells committed to the photoreceptor fate from expanded mouse retinal stem cells. Stem Cells 24: 2060-2070.
60. Comyn O, Lee E, MacLaren RE (2010) Induced pluripotent stem cell therapies for retinal disease. Current opinion in neurology 23: 4-9.

61. Zacchigna S, Oh H, Wilsch-Brauninger M, Missol-Kolka E, Jaszai J, et al. (2009) Loss of the cholesterol-binding protein prominin-1/CD133 causes disk dysmorphogenesis and photoreceptor degeneration. J Neurosci 29: 2297-2308.
62. Permanyer J, Navarro R, Friedman J, Pomares E, Castro-Navarro J, et al. (2010) Autosomal recessive retinitis pigmentosa with early macular affectation caused by premature truncation in PROM1. Invest Ophthalmol Vis Sci 51: 2656-2663.
63. Maw MA, Corbeil D, Koch J, Hellwig A, Wilson-Wheeler JC, et al. (2000) A frameshift mutation in prominin (mouse)-like 1 causes human retinal degeneration. Hum Mol Genet 9: 27-34.
64. Zhang Q, Zulfiqar F, Xiao X, Riazuddin SA, Ahmad Z, et al. (2007) Severe retinitis pigmentosa mapped to 4p15 and associated with a novel mutation in the PROM1 gene. Hum Genet 122: 293-299.
65. Pras E, Abu A, Rotenstreich Y, Avni I, Reish O, et al. (2009) Cone-rod dystrophy and a frameshift mutation in the PROM1 gene. Mol Vis 15: 1709-1716.
66. Littink KW, Koenekoop RK, van den Born LI, Collin RW, Moruz L, et al. (2010) Homozygosity mapping in patients with cone-rod dystrophy: novel mutations and clinical characterizations. Invest Ophthalmol Vis Sci 51: 5943-5951.
67. Kniazeva M, Chiang MF, Morgan B, Anduze AL, Zack DJ, et al. (1999) A new locus for autosomal dominant stargardt-like disease maps to chromosome 4. Am J Hum Genet 64: 1394-1399.
68. Michaelides M, Johnson S, Poulson A, Bradshaw K, Bellmann C, et al. (2003) An autosomal dominant bull's-eye macular dystrophy (MCDR2) that maps to the short arm of chromosome 4. Invest Ophthalmol Vis Sci 44: 1657-1662.
69. Yang Z, Chen Y, Lillo C, Chien J, Yu Z, et al. (2008) Mutant prominin 1 found in patients with macular degeneration disrupts photoreceptor disk morphogenesis in mice. J Clin Invest 118: 2908-2916.
70. Michaelides M, Gaillard MC, Escher P, Tiab L, Bedell M, et al. (2010) The PROM1 mutation p.R373C causes an autosomal dominant bull's eye maculopathy associated with rod, rod-cone, and macular dystrophy. Invest Ophthalmol Vis Sci 51: 4771-4780.
71. Allocca M, Mussolino C, Garcia-Hoyos M, Sanges D, Iodice C, et al. (2007) Novel adeno-associated virus serotypes efficiently transduce murine photoreceptors. J Virol 81: 11372-11380.

72. Pang JJ, Lauramore A, Deng WT, Li Q, Doyle TJ, et al. (2008) Comparative analysis of in vivo and in vitro AAV vector transduction in the neonatal mouse retina: effects of serotype and site of administration. Vision Res 48: 377-385.
73. Natkunarajah M, Trittibach P, McIntosh J, Duran Y, Barker SE, et al. (2008) Assessment of ocular transduction using single-stranded and self-complementary recombinant adeno-associated virus serotype 2/8. Gene Ther 15: 463-467.
74. Wang J, Faust SM, Rabinowitz JE (2011) The next step in gene delivery: molecular engineering of adeno-associated virus serotypes. J Mol Cell Cardiol 50: 793-802.
75. Boye SE, Boye SL, Pang J, Ryals R, Everhart D, et al. (2010) Functional and behavioral restoration of vision by gene therapy in the guanylate cyclase-1 (GC1) knockout mouse. PLoS One 5: e11306.
76. Acland GM, Aguirre GD, Ray J, Zhang Q, Aleman TS, et al. (2001) Gene therapy restores vision in a canine model of childhood blindness. Nature genetics 28: 92-95.
77. Ku CA, Chiodo VA, Boye SL, Goldberg AF, Li T, et al. (2011) Gene therapy using self-complementary Y733F capsid mutant AAV2/8 restores vision in a model of early onset Leber congenital amaurosis. Human molecular genetics 20: 4569-4581.
78. Pang JJ, Deng WT, Dai X, Lei B, Everhart D, et al. (2012) AAV-mediated cone rescue in a naturally occurring mouse model of CNGA3-achromatopsia. PLoS One 7: e35250.
79. Mao H, Gorbatyuk MS, Hauswirth WW, Lewin AS (2012) Gene delivery of wild-type rhodopsin rescues retinal function in an autosomal dominant retinitis pigmentosa mouse model. Advances in experimental medicine and biology 723: 199-205.
80. Gorbatyuk MS, Gorbatyuk OS, LaVail MM, Lin JH, Hauswirth WW, et al. (2012) Functional rescue of P23H rhodopsin photoreceptors by gene delivery. Advances in experimental medicine and biology 723: 191-197.
81. Pang JJ, Dai X, Boye SE, Barone I, Boye SL, et al. (2011) Long-term retinal function and structure rescue using capsid mutant AAV8 vector in the rd10 mouse, a model of recessive retinitis pigmentosa. Mol Ther 19: 234-242.
82. Beltran WA, Cideciyan AV, Lewin AS, Iwabe S, Khanna H, et al. (2012) Gene therapy rescues photoreceptor blindness in dogs and paves the way for treating human X-linked retinitis pigmentosa. Proceedings of the National Academy of Sciences of the United States of America 109: 2132-2137.
83. Corbeil D, Roper K, Hannah MJ, Hellwig A, Huttner WB (1999) Selective localization of the polytopic membrane protein prominin in microvilli of epithelial cells - a

combination of apical sorting and retention in plasma membrane protrusions. J Cell Sci 112 (Pt 7): 1023-1033.

84. Han Z, Anderson DW, Papermaster DS (2012) Prominin-1 localizes to the open rims of outer segment lamellae in Xenopus laevis rod and cone photoreceptors. Invest Ophthalmol Vis Sci 53: 361-373.
85. Wen R, Tao W, Li Y, Sieving PA (2012) CNTF and retina. Prog Retin Eye Res 31: 136-151.
86. Wen R, Tao W, Luo L, Huang D, Kauper K, et al. (2012) Regeneration of cone outer segments induced by CNTF. Adv Exp Med Biol 723: 93-99.
87. Talcott KE, Ratnam K, Sundquist SM, Lucero AS, Lujan BJ, et al. (2011) Longitudinal study of cone photoreceptors during retinal degeneration and in response to ciliary neurotrophic factor treatment. Invest Ophthalmol Vis Sci 52: 2219-2226.
88. Picard E, Jonet L, Sergeant C, Vesvres MH, Behar-Cohen F, et al. (2010) Overexpressed or intraperitoneally injected human transferrin prevents photoreceptor degeneration in rd10 mice. Mol Vis 16: 2612-2625.
89. Vasireddy V, Chavali VR, Joseph VT, Kadam R, Lin JH, et al. (2011) Rescue of photoreceptor degeneration by curcumin in transgenic rats with P23H rhodopsin mutation. PLoS One 6: e21193.
90. Shen J, Ghai K, Sompol P, Liu X, Cao X, et al. (2012) N-acetyl serotonin derivatives as potent neuroprotectants for retinas. Proc Natl Acad Sci U S A 109: 3540-3545.
91. Chen J, Patil S, Seal S, McGinnis JF (2006) Rare earth nanoparticles prevent retinal degeneration induced by intracellular peroxides. Nat Nanotechnol 1: 142-150.
92. Kovach JL, Schwartz SG, Flynn HW, Jr., Scott IU (2012) Anti-VEGF Treatment Strategies for Wet AMD. J Ophthalmol 2012: 786870.
93. Lally DR, Gerstenblith AT, Regillo CD (2012) Preferred therapies for neovascular age-related macular degeneration. Curr Opin Ophthalmol 23: 182-188.
94. Polosukhina A, Litt J, Tochitsky I, Nemargut J, Sychev Y, et al. (2012) Photochemical restoration of visual responses in blind mice. Neuron 75: 271-282.
95. Fernandes RA, Diniz B, Ribeiro R, Humayun M (2012) Artificial vision through neuronal stimulation. Neurosci Lett 519: 122-128.
96. Wilke R, Gabel VP, Sachs H, Bartz Schmidt KU, Gekeler F, et al. (2011) Spatial resolution and perception of patterns mediated by a subretinal 16-electrode array in patients blinded by hereditary retinal dystrophies. Invest Ophthalmol Vis Sci 52: 5995-6003.

97. Stingl K, Bartz-Schmidt KU, Besch D, Gekeler F, Greppmaier U, et al. (2012) [What can blind patients see in daily life with the subretinal Alpha IMS implant? Current overview from the clinical trial in Tubingen]. Ophthalmologe 109: 136-141.
98. Nirenberg S, Pandarinath C (2012) Retinal prosthetic strategy with the capacity to restore normal vision. Proc Natl Acad Sci U S A.
99. Wang L, Mathieson K, Kamins TI, Loudin JD, Galambos L, et al. (2012) Photovoltaic retinal prosthesis: implant fabrication and performance. J Neural Eng 9: 046014.
100. Rein ML, Deussing JM (2012) The optogenetic (r)evolution. Mol Genet Genomics 287: 95-109.
101. Busskamp V, Picaud S, Sahel JA, Roska B (2012) Optogenetic therapy for retinitis pigmentosa. Gene Ther 19: 169-175.
102. Bi A, Cui J, Ma YP, Olshevskaya E, Pu M, et al. (2006) Ectopic expression of a microbial-type rhodopsin restores visual responses in mice with photoreceptor degeneration. Neuron 50: 23-33.
103. Tomita H, Sugano E, Isago H, Hiroi T, Wang Z, et al. (2010) Channelrhodopsin-2 gene transduced into retinal ganglion cells restores functional vision in genetically blind rats. Exp Eye Res 90: 429-436.
104. Lin B, Koizumi A, Tanaka N, Panda S, Masland RH (2008) Restoration of visual function in retinal degeneration mice by ectopic expression of melanopsin. Proc Natl Acad Sci U S A 105: 16009-16014.
105. Lagali PS, Balya D, Awatramani GB, Munch TA, Kim DS, et al. (2008) Light-activated channels targeted to ON bipolar cells restore visual function in retinal degeneration. Nat Neurosci 11: 667-675.
106. Doroudchi MM, Greenberg KP, Liu J, Silka KA, Boyden ES, et al. (2011) Virally delivered channelrhodopsin-2 safely and effectively restores visual function in multiple mouse models of blindness. Mol Ther 19: 1220-1229.
107. Busskamp V, Duebel J, Balya D, Fradot M, Viney TJ, et al. (2010) Genetic reactivation of cone photoreceptors restores visual responses in retinitis pigmentosa. Science 329: 413-417.
108. Jacobson SG, Cideciyan AV, Ratnakaram R, Heon E, Schwartz SB, et al. (2012) Gene therapy for leber congenital amaurosis caused by RPE65 mutations: safety and efficacy in 15 children and adults followed up to 3 years. Archives of ophthalmology 130: 9-24.
109. Joe AW, Gregory-Evans K (2010) Mesenchymal stem cells and potential applications in treating ocular disease. Curr Eye Res 35: 941-952.

110. Johnson TV, Bull ND, Hunt DP, Marina N, Tomarev SI, et al. (2010) Neuroprotective effects of intravitreal mesenchymal stem cell transplantation in experimental glaucoma. Invest Ophthalmol Vis Sci 51: 2051-2059.

111. Harper MM, Grozdanic SD, Blits B, Kuehn MH, Zamzow D, et al. (2011) Transplantation of BDNF-secreting mesenchymal stem cells provides neuroprotection in chronically hypertensive rat eyes. Invest Ophthalmol Vis Sci 52: 4506-4515.

112. Baird GS, Zacharias DA, Tsien RY (2000) Biochemistry, mutagenesis, and oligomerization of DsRed, a red fluorescent protein from coral. Proceedings of the National Academy of Sciences of the United States of America 97: 11984-11989.

113. Yamaguchi M, Saito H, Suzuki M, Mori K (2000) Visualization of neurogenesis in the central nervous system using nestin promoter-GFP transgenic mice. Neuroreport 11: 1991-1996.

114. Vicidomini G, Gagliani MC, Canfora M, Cortese K, Frosi F, et al. (2008) High data output and automated 3D correlative light-electron microscopy method. Traffic 9: 1828-1838.

8) Acknowledgements

I like to thank John Wilson, PhD for rhoEGFP mice, Anand Swaroop, PhD for Nrl-EGFP mice, Profs. Thaddeus P. Dryja, Jane Farrar, and Peter Humphries for P347S mice, Jochen Haas, Susanne Kretschmar and Anne-Marie Marzesco for technical support, Carmen Friebel and Sindy Böhme for animal husbandry, Drs. Denis Corbeil, Annette Rünker and Mike Karl for helpful discussions and critically reading the manuscripts and my thesis advisory committee members Andrew C. Oates, PhD and Prof. Dr. Elly M. Tanaka for perfect supervision and fruitful discussions.

Especially, I like to thank Drs. Marius Ader, Thomas Kurth, Sandra Schubert, Stefan Weger and Prof. Regine Heilbronn, as well as Kai Postel, Tiago Santos-Ferreira and Madalena Carido since without their engagement and dedication this work would not have been possible.

Last, but not least, I like to thank my significant other, all members of my family, her family and our closest friends for being there whenever needed, for emotional backup and for the “wunderbar“ and happy times I had with them.

9) Appendix

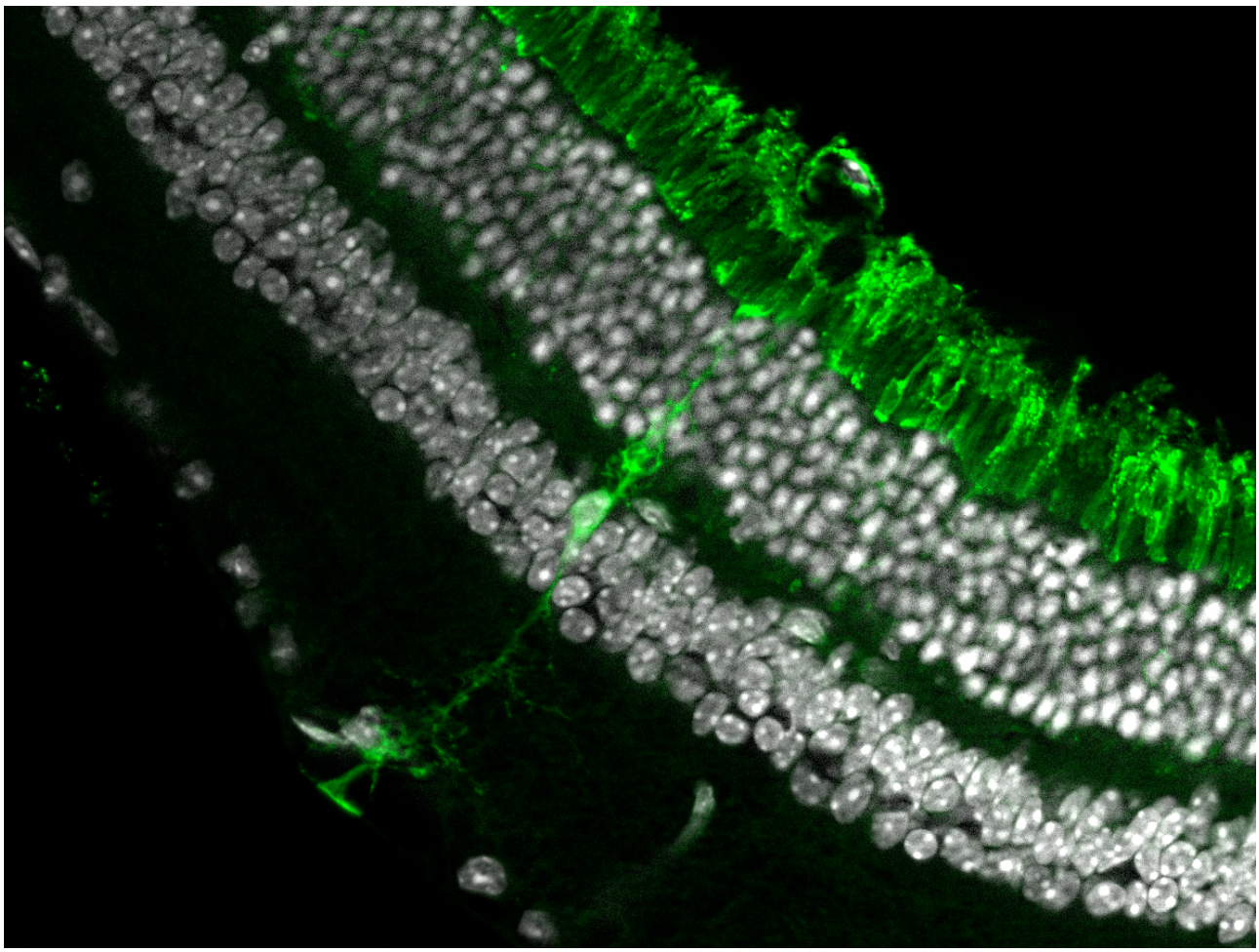

Figure S1: Other retinal cell types which might be transduced in low numbers.

Depicted here is a Müller glia cell which was transduced after sub-retinal delivery of rAAV2/5-CMV-prominin-1::GFP, expressing prominin-1::GFP transgene (green). Nuclear DAPI staining is shown in white.

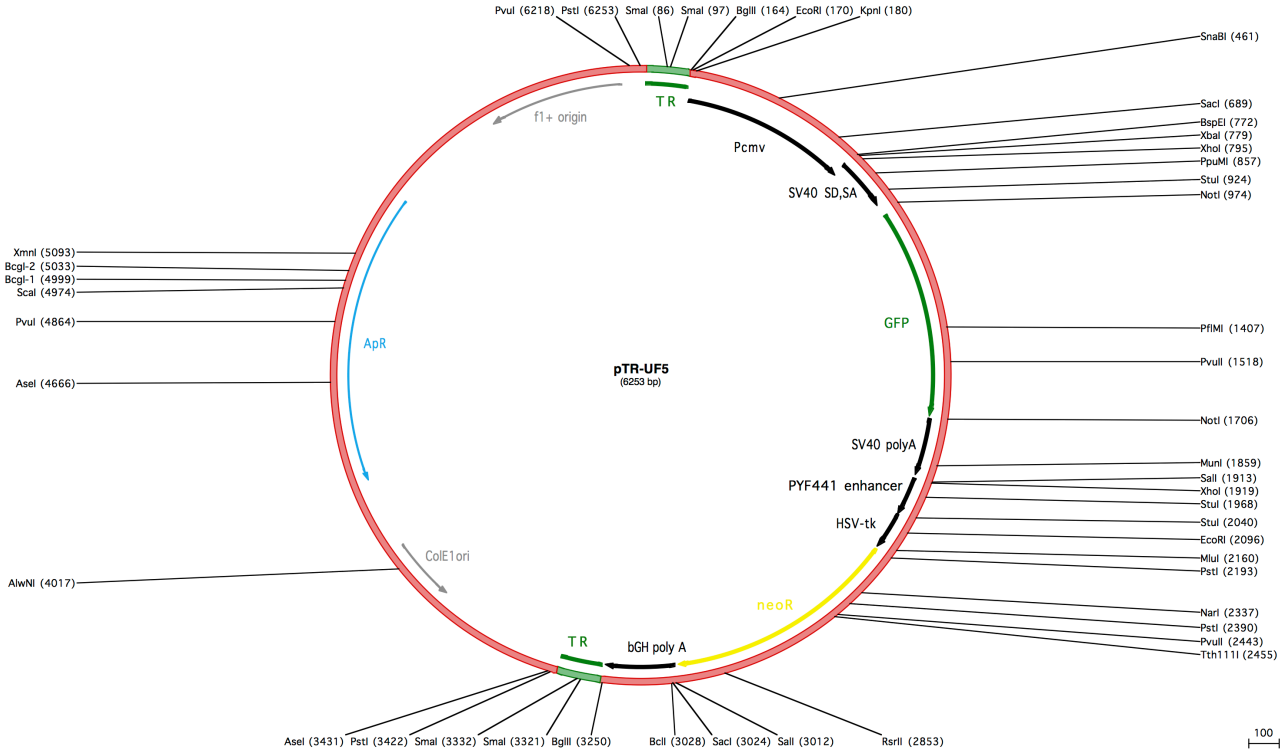

Figure S2: Vector map pTR-UF5. Monomeric vector expressing GFP used for packaging with 2/5 or 2/8 capsid.

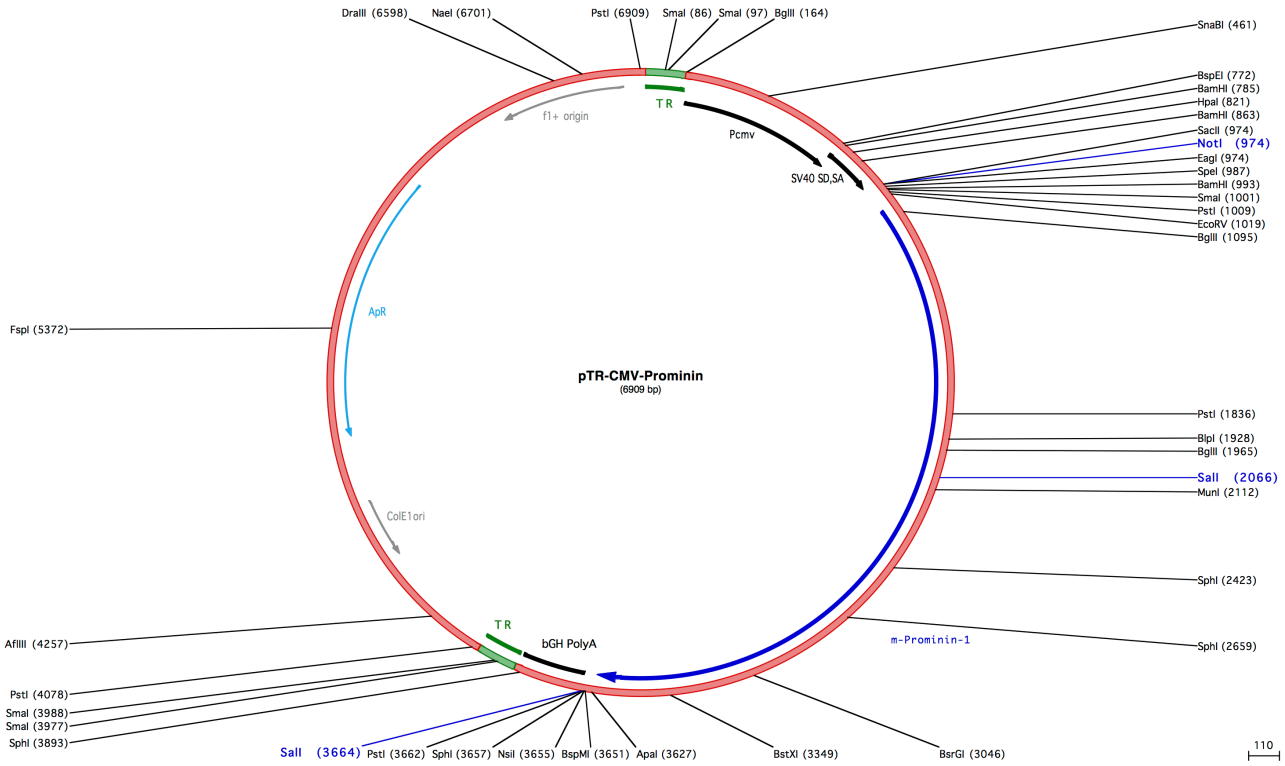

Figure S3: Vector map pTR-CMV-Prominin. Monomeric vector expressing mouse prominin-1 used for packaging with 2/8 capsid.

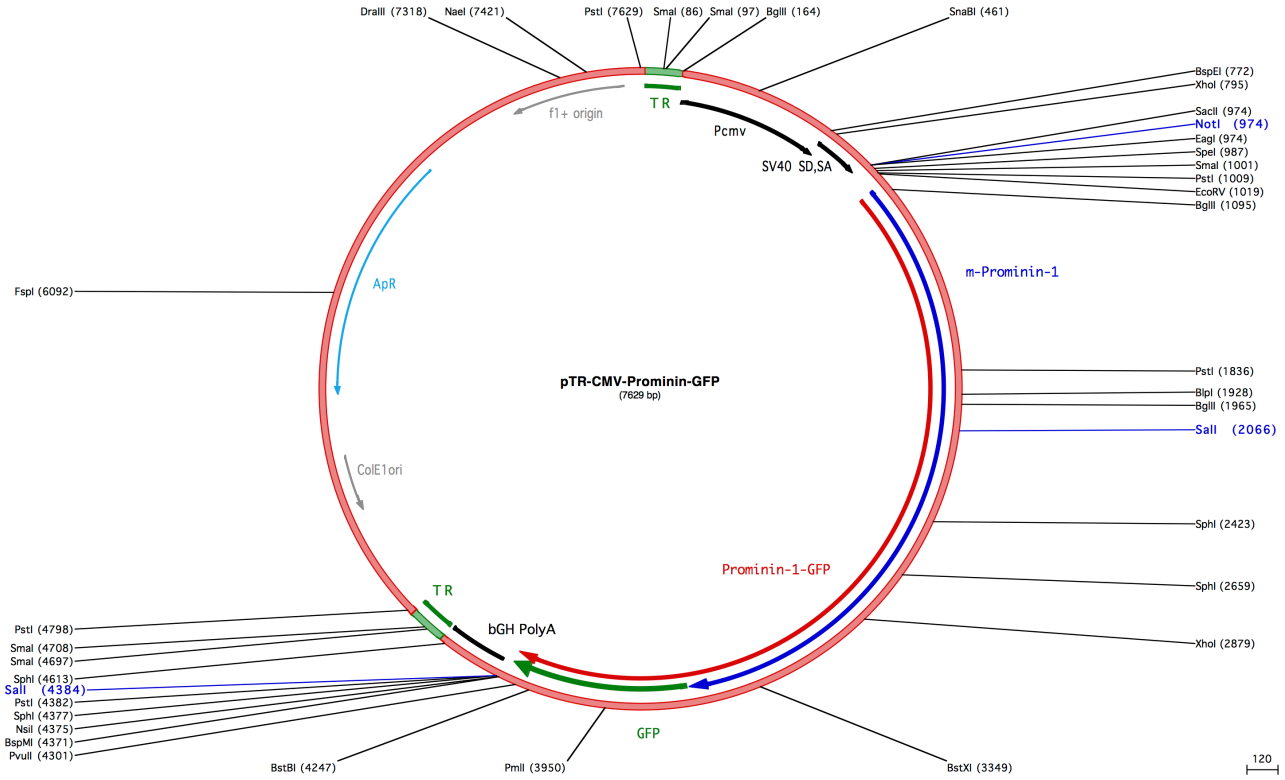

Figure S4: Vector map pTR-CMV-Prominin-GFP. Monomeric vector expressing prominin-1::GFP fusion protein used for packaging with 2/5 capsid.

Erklärung entsprechend §5.5 der Promotionsordnung

Hiermit versichere ich, dass ich die vorliegende Arbeit ohne unzulässige Hilfe Dritter und ohne Benutzung anderer als der angegebenen Hilfsmittel angefertigt habe. Die aus fremden Quellen direkt oder indirekt übernommenen Gedanken sind als solche kenntlich gemacht. Die Arbeit wurde bisher weder im Inland noch im Ausland in gleicher oder ähnlicher Form einer anderen Prüfungsbehörde vorgelegt.

Die Dissertation wurde im Zeitraum vom 15.10.2008 bis 05.09.2012 verfasst und von Prof. Dr. Elly M. Tanaka, Center for Regenerative Therapies, TU Dresden betreut.

Meine Person betreffend erkläre ich hiermit, dass keine früheren erfolglosen Promotionsverfahren stattgefunden haben.

Ich erkenne die Promotionsordnung der Fakultät für Mathematik und Naturwissenschaften, Technische Universität Dresden an.

_____

Dresden, 05.09.2012